FATİH UNIVERSITY

The Graduate School of Sciences and Engineering

**Doctor of Philosophy in
Electrical and Electronics Engineering**

**DEVELOPMENT OF A WIDEBAND DIRECTION
FINDING SYSTEM**

by

Mehmet Emin ÖZTÜRK

February 2016

DEVELOPMENT OF A WIDEBAND DIRECTION FINDING SYSTEM

by

Mehmet Emin ÖZTÜRK

A thesis submitted to

the Graduate School of Sciences and Engineering

of

Fatih University

in partial fulfillment of the requirements for the degree of

Doctor of Philosophy

in

Electrical and Electronics Engineering

February 2016
Istanbul, Turkey

APPROVAL PAGE

This is to certify that I have read this thesis written by Mehmet Emin ÖZTÜRK and that in my opinion it is fully adequate, in scope and quality, as a thesis for the degree of Doctor of Philosophy in Electrical and Electronics Engineering.

_____

Assoc. Prof. Erdal KORKMAZ
Thesis Supervisor

I certify that this thesis satisfies all the requirements as a thesis for the degree of Doctor of Philosophy in Electrical and Electronics Engineering.

_____

Prof. Onur TOKER
Head of Department

Examining Committee Members

Prof. Bayram ÜNAL   _____

Assoc. Prof. Erdal KORKMAZ   _____

Assoc. Prof. Salih DEMİREL   _____

Asst. Prof. Hüseyin SAĞKOL   _____

Asst. Prof. Saime AKDEMİR AKAR   _____

It is approved that this thesis has been written in compliance with the formatting rules laid down by the Graduate School of Sciences and Engineering.

_____

Prof. Nurullah ARSLAN
Director

February 2016

DEVELOPMENT OF A WIDEBAND DIRECTION FINDING SYSTEM

Mehmet Emin ÖZTÜRK

Ph.D. Thesis – Electrical and Electronics Engineering
February 2016

Thesis Supervisor: Assoc. Prof Erdal KORKMAZ

ABSTRACT

Relatively small wideband antenna is designed and manufactured for the mobile application of direction finding systems for the frequency range from 150 MHz to 3 GHz. The proposed directional wideband antenna is a rounded-edge directed bow-tie antenna which is electrically small when considering at lower operating frequencies. A good agreement is obtained between the simulation and measurement results of the designed antenna. The performance of the antenna for direction finding applications is verified both in anechoic chamber measurements and in open field measurements. In addition, in open field direction finding measurements the proposed antenna is compared with a commercial antenna. During the tests, one of the angle of arrival estimation technique based on phase differences of the signal at the antenna elements, interferometer method, and combination of the phase differences and amplitude values of the captured signal were used. As well as, k-means clustering used to reduce undesired error due to environmental effects.

Keywords: Direction Finding, Angle of Arrival, Interferometer.

GENİŞ BANTLI YÖN BULMA SİSTEMİNİN GELİŞTİRİLMESİ
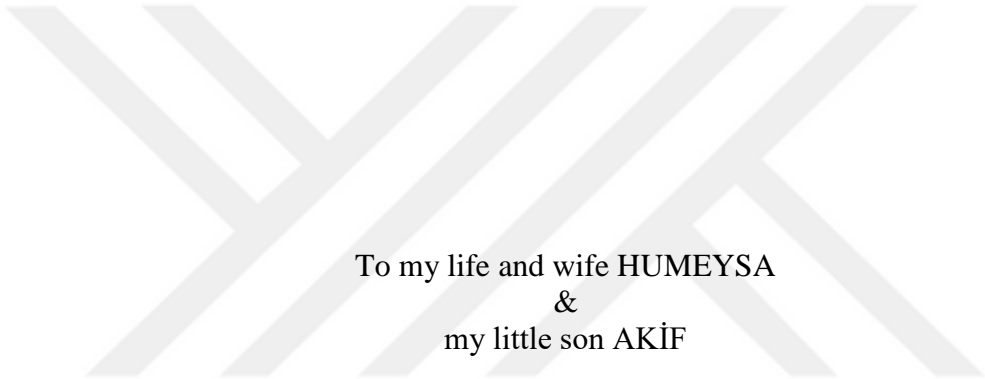
Mehmet Emin ÖZTÜRK

Doktora Tezi – Elektrik ve Elektronik Mühendisliği
Şubat 2016

Tez Danışmanı: Doç. Dr. Erdal KORKMAZ

ÖZ

Yön bulma sistemlerinin mobil uygulamaları için 150 MHz'den 3 GHz'e kadar frekans aralığında çalışabilen nispeten küçük geniş band anten tasarlanmış ve üretilmiştir. Önerilen anten yönlü geniş bantlı bir anten olup, çalıştığı en düşük frekans göz önüne alındığında elektriksel olarak küçük boyutlarda kenarları yay şeklinde papyon antendir. Tasarlanan antenin simülasyon ve ölçüm değerleri birbiri ile örtüşmektedir. Antenin performansı hem tam yansımasız odada hem de açık alanda yapılan ölçümlerle doğrulanmıştır. Ayrıca, ticari bir yön bulma anteni ile kıyaslanma yapılmıştır. Testler sırasında, yakalanan sinyalin faz farkına dayalı olan interferometri yöntemi ile birlikte genlik bilgisi ve faz bilgisinin birlikte kullanıldığı yön bulma algoritmaları kullanıldı. Yanı sıra, k-ortalama kümesi istenmeyen çevresel etkilerden oluşan hataları azaltmak için kullanıldı.

Anahtar Kelimeler: Yön Bulma, Varış Açısı, İnterferometri.

To my life and wife HUMEYSA
&
my little son AKİF

ACKNOWLEDGEMENT

TABLE OF CONTENTS

LIST OF FIGURES

LIST OF SYMBOLS AND ABBREVIATIONS

SYMBOL/ABBREVIATION

AoA	Angle of Arrival
COMINT	Communication Intelligence
DBTA	Directed Bow-Tie Antenna
DF	Direction Finding
DFT	Discrete Fourier Transform
DREBT	Directed Rounded-Edge Bow-Tie
EKF	Extended Kalman Filter
EOB	Electronic Order of Battle
ESM	Electronic Support Measures
FM	Frequency Modulation
GPS	Global Positioning System
HF	High Frequency
IF	Intermediate Frequency
KF	Kalman Filter
MHz	Mega Hertz
MUSIC	Multiple Signal Classification
PLL	Phase-Locked Loop
RF	Radio Frequency
SNR	Signal to Noise Ratio
UHF	Ultra-High Frequency
UPS	Uninterruptible Power Supply
VHF	Very-High Frequency
λ	Wave Length

CHAPTER 1

INTRODUCTION

In literature, direction finding (DF) is described as determining the location of radio transmission sources. In practically, DF covers the locating, tracking and distinguishing the different radio transmissions sources.

1.1 BACKGROUND OF DIRECTION FINDING SYSTEMS

DF studies were begun during the early years of the nineteenth century with the work performed by Hertz, Marconi and Zenneck on directive antennas. The first experiments in this field are made by Marconi in 1906. When a directional antenna was rotated 360 degrees on the azimuthal plane, the peak amplitude of the incoming signal occurs at the angle of arrival (AoA) that is an angle of source transmission with respect to DF system (Jenkins, 1991).

Immediately after the World War I, enormous developments were made in DF technology hand in hand with the great improvements in the general vacuum-tube based radio technology. In spite of the fact that these early DF systems were very simplistic with respect to today's DF technology, nevertheless they founded the fundamental structures of today's advanced DF systems. The methods used in the DF systems started by simply turning a directive antenna 360 degrees and have been developed using multiple-antenna array and complex computer algorithms over the last century to find the direction of arrival of incoming radio frequency (RF) signals (Bailey et al., 2012).

The needs of the both World Wars inspired the major advances in direction finding technology. Until the end of the World War II, the direction finding was focused on the high frequency (HF) band, 0.5-30 MHz, due to the fact that at that time long range telecommunication could not be achieved in another way at. Between both World Wars, very crucial developments in DF area had been achieved (Liberal et al., 2011).

Several developments in electronics during and after the World War II led to greatly improved methods of comparing the phase of signals. In addition, the phase-locked loop (PLL) allowed for easy tuning in signals, which wouldn't drift. Improved vacuum tubes and the introduction of the transistor allowed much higher frequencies to be used economically, which led to widespread use of very-high frequency (VHF) and ultra-high frequency (UHF) signals. All of these changes led to new methods of DF, and much more widespread usage (Liang and Chia, 2001).

After 1980s, super resolution algorithms had begun to be studied. Multiple Signal Classification (MUSIC) was applied to the DF algorithms by Schmidt at 1986. Super resolution methods are candidates to find the AoA of signals at the same frequency which the classical techniques cannot resolve. However, super resolution algorithms cannot be used for wideband applications (Lim et al., 2010).

1.2 APPLICATIONS OF DIRECTION FINDING SYSTEMS

DF has widespread use in numerous application areas. DF systems are primarily used by military, civilian, government and research centers (Cho et al., 2010).

Air and marine navigation, search and rescue, landing-drop-zone location, drop-zone assembly, personnel and vehicle locators, emission control, frequency management, communication intelligence (COMINT), electronic order of battle (EOB), electronic support measures (ESM), emitter homing and locating, friendly force location, force strength assessments, interference source location, emergency beacon location, wildlife tracking, spectrum monitoring, spectrum density calibrations, advanced COMINT investigations, radio noise definitions, electromagnetic studies of

severe weather and remote environmental sensing are major areas of DF system usage (Kellogg et al., 2007).

Direction finding systems can be also classified in three basic categories according to the aim of use:

- Early Warning Threat Detection
- Targeting, Homing, and Jamming
- Electronic Intelligence

1.3 MOTIVATIONS OF THE THESIS

A DF system basically consists of the antenna array, DF receiver, DF processor and display of the bearing angle. The most important part of the system is the antenna array. For mobile applications, the antenna must be small and wideband (Jahoda, 2007). Performance of the system is becoming more important in designing wideband mobile DF systems. A DF antenna system is an array antenna consists of usually an odd number of multiple antenna elements in a circular form (Kebeli, 2011). Generally, omnidirectional antennas such as dipole, monopole and bi-conical antennas (Kenddey and Sullivan, 1995) have been used as a DF antenna element. However, these antennas cannot be used over a wideband frequency range. AoA estimation algorithms use voltage values induced at the array antennas. By using of a circular arrangement of DF antenna array it is possible to use both amplitude and phase information at each single antenna elements by means of AoA estimation algorithms. Most DF systems have been using correlative interferometer technique to estimate AoA (Park and Kim, 2006). This method determines the angle of incidence signal by directly measuring the phase difference of the wave by sampling the incidence signal with elements of a DF antenna array.

The aim of the thesis is the development of an improved mobile compact wideband antenna system which is designed and implemented for the interferometric DF system. In this thesis, a relatively small novel wide band antenna is proposed as a single antenna element of a DF array which is integrated onto a vehicle-mounted mobile DF system operating over a frequency range between 150 - 3.000 MHz. The

adequateness of the proposed antenna for a mobile DF system is verified both in an anechoic chamber and in open field by using of phase differences of the signal at the antenna elements, interferometer method, and combination of the phase differences and amplitude values of the captured signals. In addition the performance of the proposed antenna is also compared under the same conditions with a commercial antenna which is widely used for DF applications. In addition MUSIC algorithm (Vaseghi, 2001) is also described and discussed.

1.4 CONTRIBUTIONS OF THE THESIS

In chapter 2, DF methods that are commonly used are described with their benefits and backwards.

In chapter 3, DF system components and used algorithms are described and analyzed in detail. Wideband DF antenna is designed and verified.

In chapter 4, proposed wideband DF system is simulated and tested both indoor and outdoor environments. Meantime, measurement results are discussed.

In chapter 5, MUSIC algorithm is developed and implemented.

In chapter 6, conclusion is given. Outcomes of the measurement results are discussed.

CHAPTER 2

DIRECTION FINDING METHODS

DF methods can be categorized by amplitude comparison based, phase comparison based and super resolution methods.

In amplitude comparison based DF systems at least three antennas are located in such a manner that each angle of arrival of the incident wave creates unique amplitude difference between the antennas. By appropriately analyzing these amplitudes, direction of arrival of the incident wave can be calculated. Watson-Watt DF method is the most commonly used one in the amplitude comparison based DF methods (Pascal, 2000).

Doppler DF systems and interferometer based DF methods are the fundamental types of the phase comparison based DF methods. Similar to amplitude based methods, in phase comparison based DF methods, minimum three antennas are located in such a manner that each angle of arrival of the incident wave creates unique phase differences between the antennas. By using these phase differences, direction of arrival of the incident wave is estimated (Saraç, 2009).

Furthermore, with the advance of the DF technology super resolution methods are introduced like Beamforming and sub-space methods (Wu, 1991).

2.1 AMPLITUDE BASED DIRECTION FINDING METHODS

2.1.1 Watson-Watt Method

As mentioned above, the Watson-Watt DF method is one of the amplitude

comparison DF methods. Generally, Watson-Watt DF systems use either Adcock or loop antennas while Adcocks are usually preferred because of their excellent performance. Essentially, the Adcocks antenna is an array of three separate antennas. Referring to a 4-aerial Adcock configuration, the first group of these antennas is the N-S bi-directional array comprising the North and South aerials as depicted in Fig. 2.1. To produce the Y-axis voltage, N and S aerial vectoral voltages are subtracted. The second group of these antennas is the E-W bi-directional array comprising the East and West aerials. This pattern is repeatedly determined by applying the E and W aerial voltages to a differencing network that subtracts them vectorially (E-W) to produce what will ultimately become the X-axis voltage. Fig. 2.1 shows the azimuthal gain patterns of an Adcock DF antenna used for implementation of Watson Watt Method (Yeo and Lee, 2012).
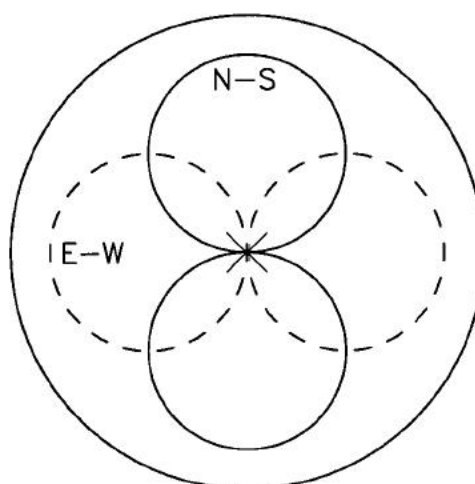
Figure 2.1 Azimuthal gain patterns of Adcock DF antenna used for Watson-Watt Method.

The third group of these antennas is the omni-directional sense antenna. The sense antenna is required to resolve an 180° ambiguity that would otherwise result. Since the Watson-Watt DF technique falls into the amplitude-comparison category as discussed above, the purpose of the remaining components of the DF system (i.e., the DF receiver, DF bearing processor, and DF bearing display) is simply to measure the X- and Y-axis

voltages and then compute and display the bearing. They can therefore be mapped into a corresponding bearing using an appropriate algorithm that performs a computation based on their ratio (Yong et al., 2001).

2.2 PHASE BASED DIRECTION FINDING METHODS

2.2.1 Doppler Method

The concept of the Doppler DF system is inspired from the "Doppler Effect" which is defined by the Austrian physicist Christian Doppler in 1842. Doppler Effect is the change in the frequency of a wave coming from a moving source relative to an observer. If the moving source is being closer, the relative frequency of the wave becomes higher, in the same way, as the moving source is being farther; the relative frequency of the wave becomes lower (Wax and Sheinvald, 1994).

Doppler Effect is directly proportional to the relative speed of the source and the receiver. As the speed of the relative movement increases the Doppler Effect at the frequency also increases (Pierre and Kaveh, 1991).

Doppler Effect for radio frequency signals can be observed as the RF transmitter approaches to the RF receiver, the frequency seen by the receiver side becomes higher than the actual frequency transmitted by the transmitter. As the RF transmitter goes far away from the RF receiver, the frequency seen by the receiver side becomes lower than the actual frequency transmitted by the transmitter. Thus, the frequency appearing at the receiver side is dependent to the relative movements of the receiver and the transmitter (Zhou et al., 2011).

By using this phenomenon in DF area, the paper written by Earp and Godfrey of Standard Telephones and Cables, Ltd in 1947 was the first formal introduction of the Doppler DF system (Ozer, 2000).

The first Doppler DF systems made use of the Doppler Effect by using a turntable and an antenna on it. The turntable is rotated at a constant high speed. As the antenna
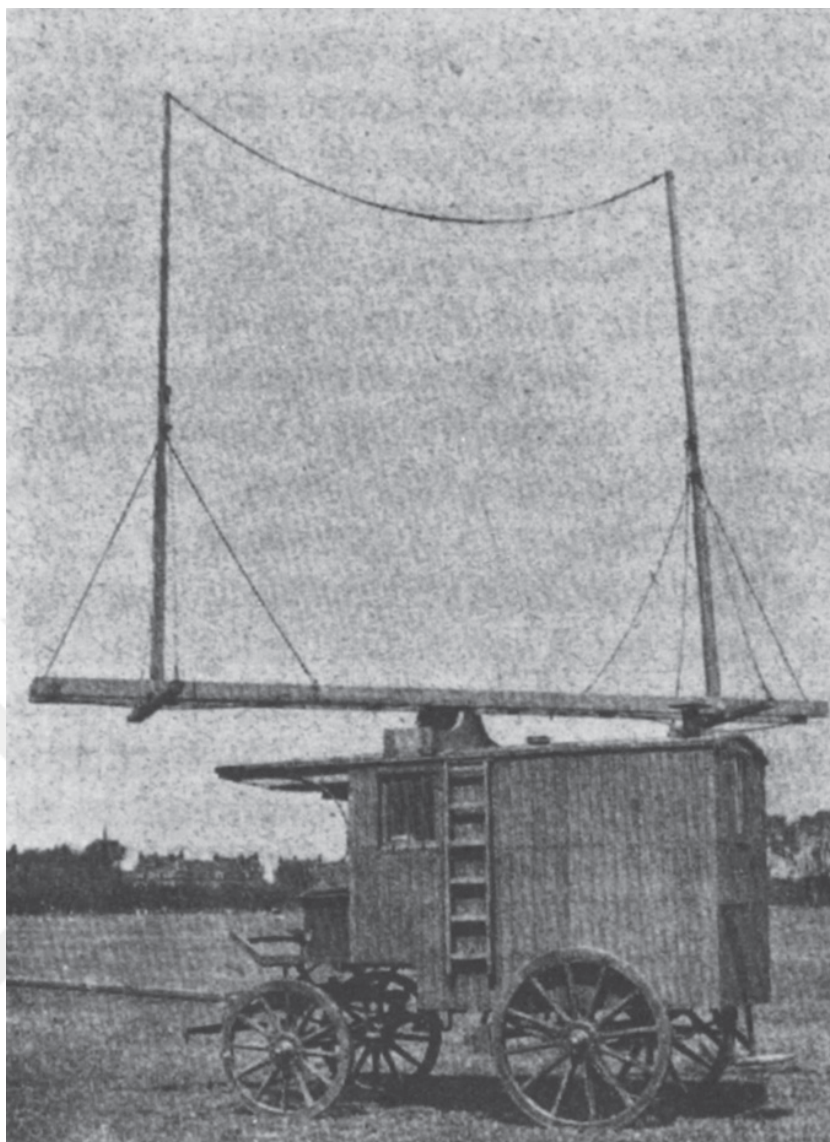
Figure 2.2 Mobile rotating-loop direction finder for military use (about 1918).

approaches to the incident signal source, the frequency received by the antenna increases. In a similar manner, as the antenna moves in a reverse direction to the incident signal source, the frequency received by the antenna decreases. The output of the antenna has a frequency modulated tone at the frequency of the rotation. The output of the antenna is connected to a frequency modulation (FM) demodulator. FM demodulator output will be the same tone with the rotational frequency. The only difference is the phase differences of the tones. This phase difference is used to find the angle of arrival (Paulraj and Kailath, 1985).
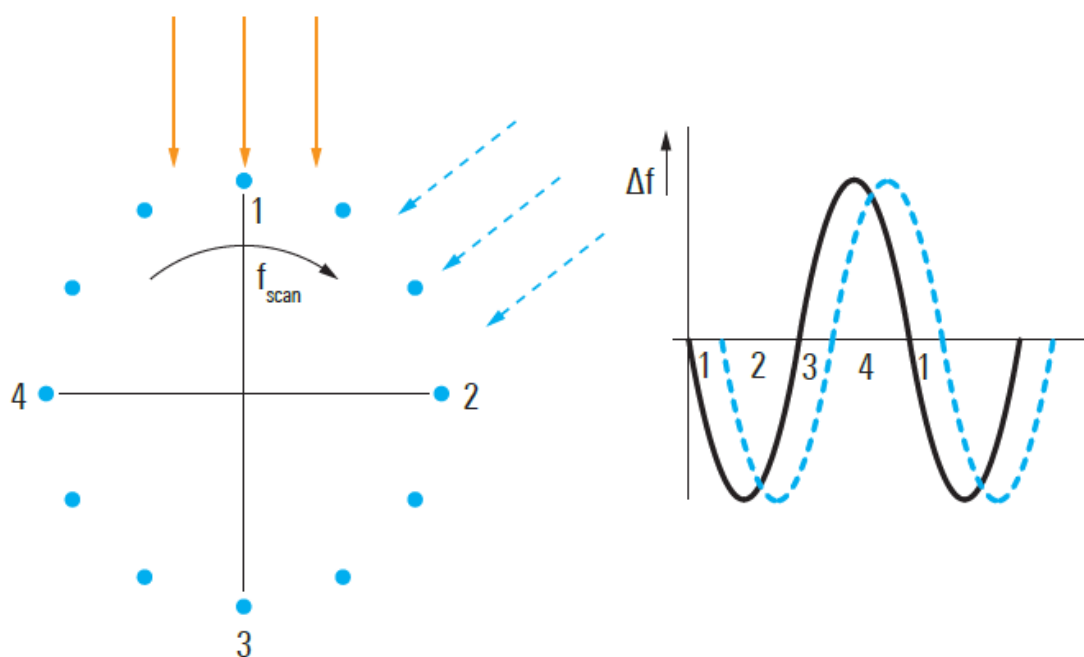
Figure 2.3 Principle of Doppler DF Method.

2.2.2 Interferometer Method

In literature, interferometer and phase interferometer methods refers to the same method. Interferometer method depends on the phases of the incident wave signal at different antennas. Since the Doppler method also depends on the phases of the received signal at distinct antennas, Doppler method is also accepted as single channel implementation of interferometer method. Basically, an antenna array consist of three or more antennas that are disposed horizontally in an appropriate manner is used as the antenna system of an interferometer DF system (Sandler and King, 1994). The outputs of these antennas are connected to phase coherent identical receiver system. Phase coherency of the receivers may be the most important point while implementing a phase dependent DF system. This receiver system takes RF signals from antennas and converts them to a lower Intermediate Frequency (IF) for the convenience of the following processing. The outputs of the phase coherent receiver systems are fed to DF processor that first determines the phase differences between the signals and then calculates the angle of arrival of the incident wave signal (Mueller et al., 2009).

The real condition of the travelling signal from transmitter to antennas is shown in Fig. 2.4 (a). If the transmitter is sufficiently far away, we can assume that d1 and d2 are parallel to each other as shown in Fig. 2.4 (b).
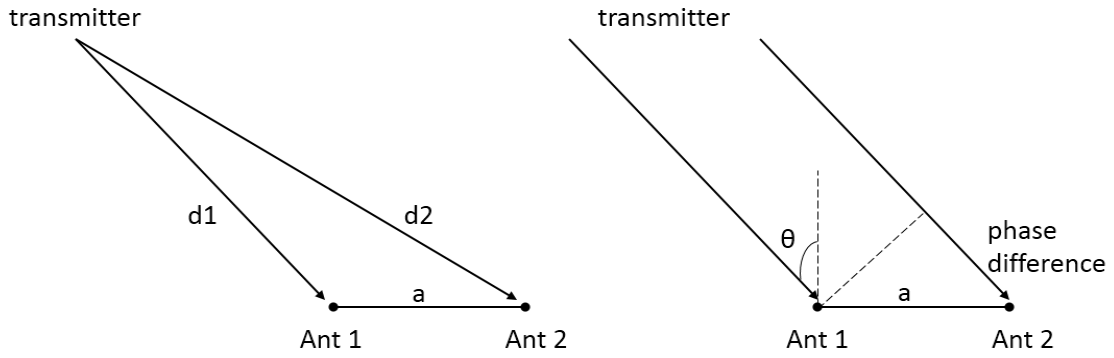
Figure 2.4 Geometry of two antenna phase comparison of a DF system (a) actual state (b) assumed state.

Phase difference, $\Delta\Phi$, is mapped from AoA for antenna separation a and incident wavelength λ by

$$\Delta\Phi = (2\pi a / \lambda)\sin\theta \tag{2.1}$$

The AoA, θ, can be calculated from Eq. (1) as:

$$\theta = \sin^{-1}(\Delta\Phi\lambda / 2\pi a) \tag{2.2}$$

The distance between receiving antennas a, in DF antenna array must be chosen carefully. For an unambiguous AoA estimation, a should be smaller than the half wavelength of the highest frequency of the incident wave if not multiple AoA's can produce the same phase difference in multiples of 2π. On the other hand, smaller antenna distances a decreases the phase resolution for the lower frequencies and increase AoA errors (Mueller et al., 2010).

Interferometer type DF systems are elegant systems and have many advantages over other DF systems like as more accuracy, high bandwidth, and higher speeds. In

addition, while All DF systems suffer from multi-path effects caused by the environmental conditions, like reflection of towers, buildings, power lines and other structures, interferometer method has an important advantage over other methods that can minimize the environmental multi-path effects by using wide aperture antenna arrays (Saraç et al., 2008a).

As the antenna aperture increases over half of the incoming wave signal's wavelength, it causes ambiguity to find the true direction of arrival that cannot be resolved easily. One method to resolve this ambiguity is to use different antenna apertures in the antenna array that minimally one of the antenna apertures is always shorter than the half of the incident wave's wavelength (Shan et al., 1985).

2.3 SUPER RESOLUTION DIRECTION FINDING METHODS

Super resolution methods are candidates to find the AoA of signals at the same frequency. Classical techniques cannot resolve this case. Since these algorithms use the data taken from the antenna array, they are classified in Array Processing techniques like beamforming. Multiple Signal Classification (MUSIC) and Beamforming are the well-known examples of high resolution direction finding methods (Thomas and Matties 2001).

2.3.1 Beamforming

This method depends on measuring the power of the incident wave at each angle of arrival. The direction of arrival estimation is done by selecting the angle of arrival where the maximum power is achieved (Le-ngoc and Le-ngoc, 1990). The power measurement at each angle of arrival is carried out by forming a beam in each angle and setting the beamformer weights equal to the corresponding steering vector at the same angle.

The array output of a beamforming system is given by:

$$y[n] = \sum_{k=0}^{N-1} \omega_k x_k[n] \qquad (2.3)$$

where $x_k[n]$ is the received signal at instant $[n]$, ω_k is the weighting vector of the beamformer, N is the number of antenna elements in the antenna array. By setting $\omega = [\omega_1, \omega_2, ...\omega_n]^T$, $x_n = [x_1[n], x_2[n], ...x_N[n]]^T$, (2.3) can be represented as

$$y[n] = \omega^h x_n \qquad (2.4)$$

Thus, the power at each angle of arrival can be calculated by

$$P(\theta) = E\left[\left|\omega^h x_n\right|^2\right] \qquad (2.5)$$

$P(\theta)$ will have maxima's at the angles where the corresponding steering vectors are equal to the beamformer weights. AoA resolution can be increased only by increasing the number of the antennas in the antenna array. The main problem here is that the weight vector has large side lobes. Although the main lobe has narrow width, the large side lobes cause more power to enter in different angle of arrivals and decreases the resolution of AoA estimation (Tan and Zhang, 1998).

2.3.2 Multiple Signal Classification

MUSIC is also called subspace based method. When there is only a single source there is no difference in performance between the amplitude based DF methods, phase based DF methods and super resolution techniques. However, when there is more than one source super resolution techniques perform significantly better than other DF methods.

MUSIC algorithm depends on separating the outputs of the antenna array into two subspaces, namely signal subspace and noise subspace. To do this separation, the method should have to estimate the noise subspace correctly. If the noise subspace is precisely estimated, it will be orthogonal to the signal subspace. In order to determine the steering vectors orthogonal to the noise subspace, MUSIC proposes to search all possible steering vectors. For orthogonality, we have

$$a(\theta)^H Q_n = 0 \qquad (2.6)$$

where $a(\theta)$ is the steering vector and Q_n is the noise subspace.

The errors in estimating the noise subspace causes $a(\theta)$ not to be precisely orthogonal to noise subspace. The function referred as the MUSIC spectrum is defined by Schmidt as

$$P_{MUSIC} = \frac{1}{a(\theta)^H Q_n Q_n^H a(\theta)} \qquad (2.7)$$

When θ is equal to the direction of arrival of one of the incoming signals, this function results in very large values. Thus, AoA estimations of the incoming signals are made by using the MUSIC spectrum (Schmidt, 1986).

CHAPTER 3

DEVELOPMENT OF A DIRECTION FINDING SYSTEM

3.1 STRUCTURE OF A DIRECTION FINDING SYSTEM

A DF system depicted with its essential components in Fig. 3.1 consists of an antenna array, a receiving system, a DF processor and a display. Antenna array serves to collect energy from the arriving signal to be used for the determination of AoA. A receiving system can be one to (n) channels synchronous receiver. Because of the expanses of increased number of channels we used two channels receiver that have analog-to-digital converters. DF processor is a controller that can be a computer which runs AoA algorithm. Display is a screen that simply shows calculated AoA.

As mentioned early, in many applications the array is generally in circular form with omni-directional antennas. Since the single antenna element that we have developed is a directional antenna there is a need for an omni-directional reference antenna to serve for the detection of interested signal (Ozturk and Kebeli, 2013b). If the frequency of the target signal source is known, reference antenna is not needed. However, in realty interested frequencies is also unknown and, it has to be found by searching the spectrum of doubted frequencies interval. It's important that the reference antenna should be an omni-directional antenna to catch the same signal strength for all possible positions of the target signal source. We did use a bi-conical antenna operating at the interested frequency band as a reference antenna. The antenna array configuration of the mobile DF system is depicted in Fig. 3.2. The number of DF array antenna is chosen 9 due to the physical limitations.
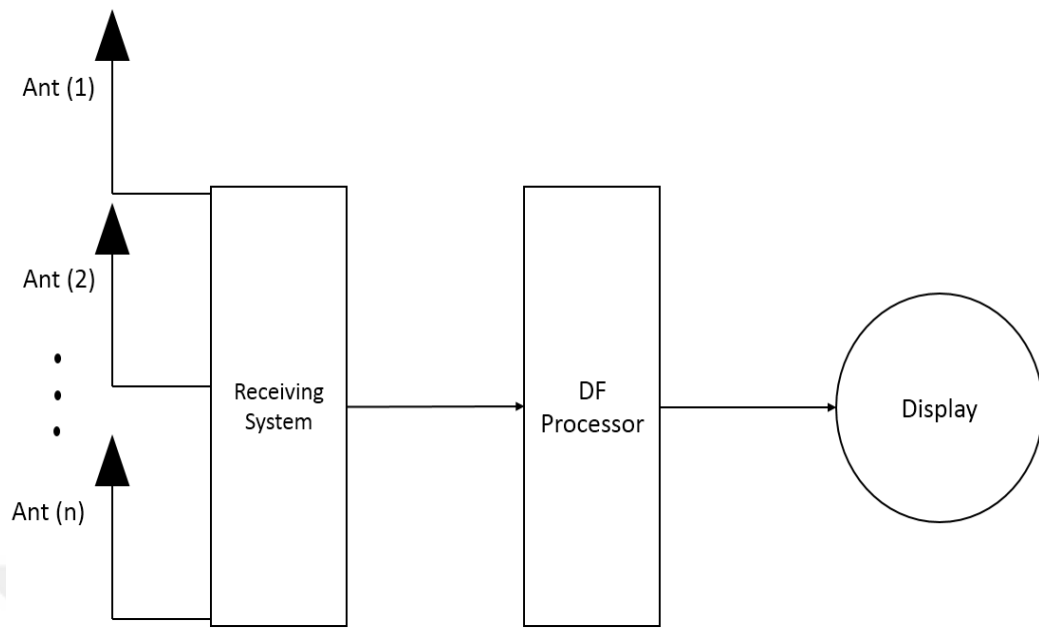
Figure 3.1 Essential components of a DF system.
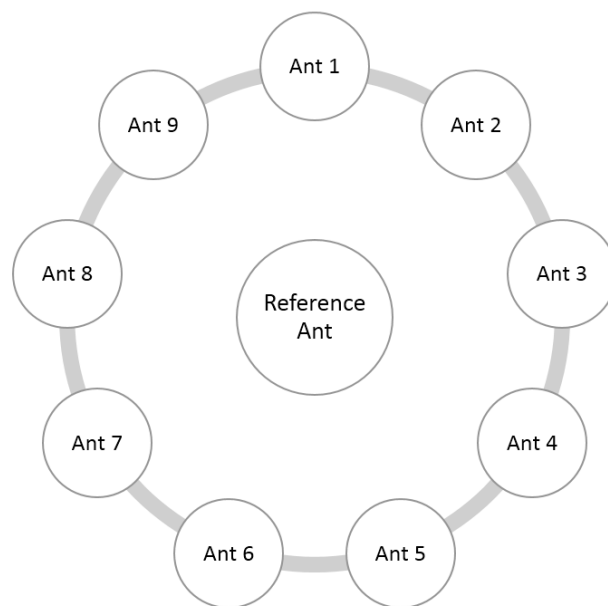
Figure 3.2 Array antenna configuration of a DF system.

3.2 HARDWARE OF A DIRECTION FINDING SYSTEM

Hardware of a DF system basically consists of the following subsystems:

1. An Antenna Array
2. DF Receivers
3. A DF Processor
4. GPS and Compass
5. Display

An antenna array is used to capture the signal at the interested frequency range. DF receivers are used to collect data conversion from RF to IF. Then, DF processor that is a computer computes the AoA with respect to data coming from GPS and compass. After that, display is used to show results both on a digital map and in numerical values.

3.2.1 Development of a Wideband Direction Finding Antenna

Because of its benefits of directed radiation pattern at all frequencies, especially in high frequencies directed Bow-Tie Antenna (DBTA) is used for direction finding system (Karacolak and Topsakal, 2006). Loaded bi-conical antenna is developed for monitoring purposes. Monitoring antenna is needed because other directed antennas are used for direction finding.

3.2.1.1. Directed Rounded-Edge Bow-Tie Antenna

Throughout the course of the research different types of DBTA are designed, simulated and measured. As seen in Fig. 3.3, used DBTA types are triangular, rounded-edge and rounded-side with rounded-edge. Length of the arm and angle between two arms are optimized with HFSS simulation program. One arm of the antenna is 25cm length with 0.1cm port height. The angle between two arms is 60 degrees (Ozturk and Kebeli, 2013a).

(a) (b) (c)
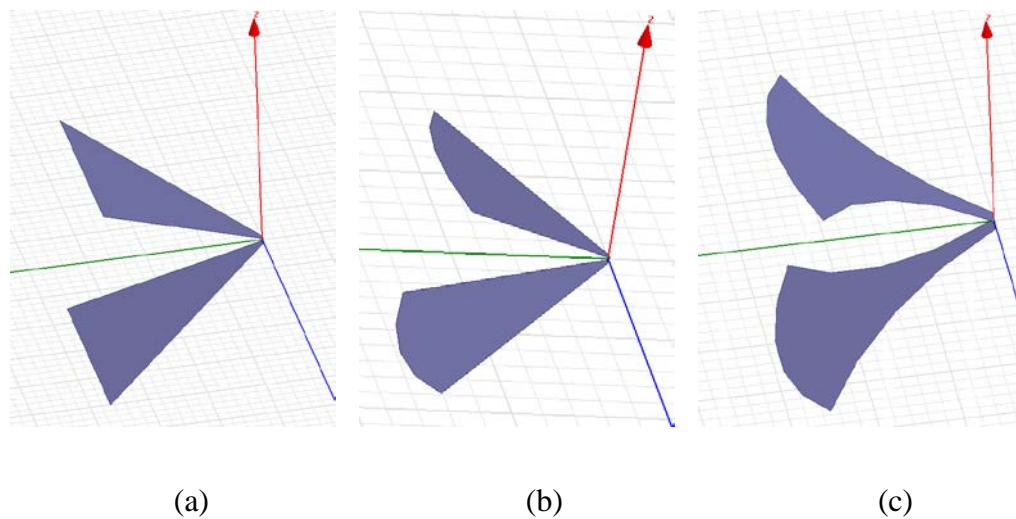
Figure 3.3 (a) Triangular DBTA, (b) Rounded-edge DBTA, (c) Rounded-side with rounded-edge DBTA.
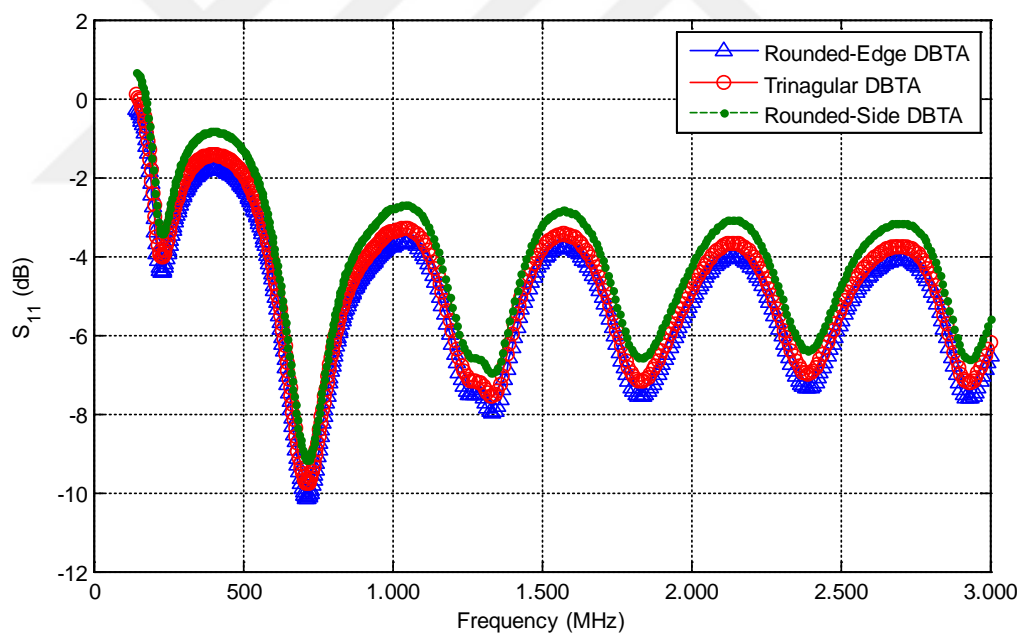
Figure 3.4 Return Loss of the Triangular DBTA, Rounded-edge DBTA and Rounded-side with rounded-edge DBTA.

DBTA is manufactured from two triangular piece of metal as shown in Fig. 3.3 (a), (b) and (c). Since we will use the antennas only in receiving mode and the demand on a wideband antenna over the frequency range makes the return loss values depicted in Fig. 3.4 satisfactory for a receiving wide band antenna. Types of the DBTA characteristics are similar. It's clear that, DREBT is slightly better over other two types as seen in Fig. 3.4. Also, its radiation pattern, especially at high frequencies is directional as shown in Fig. 3.5.

(a)   (b)

(c)   (d)
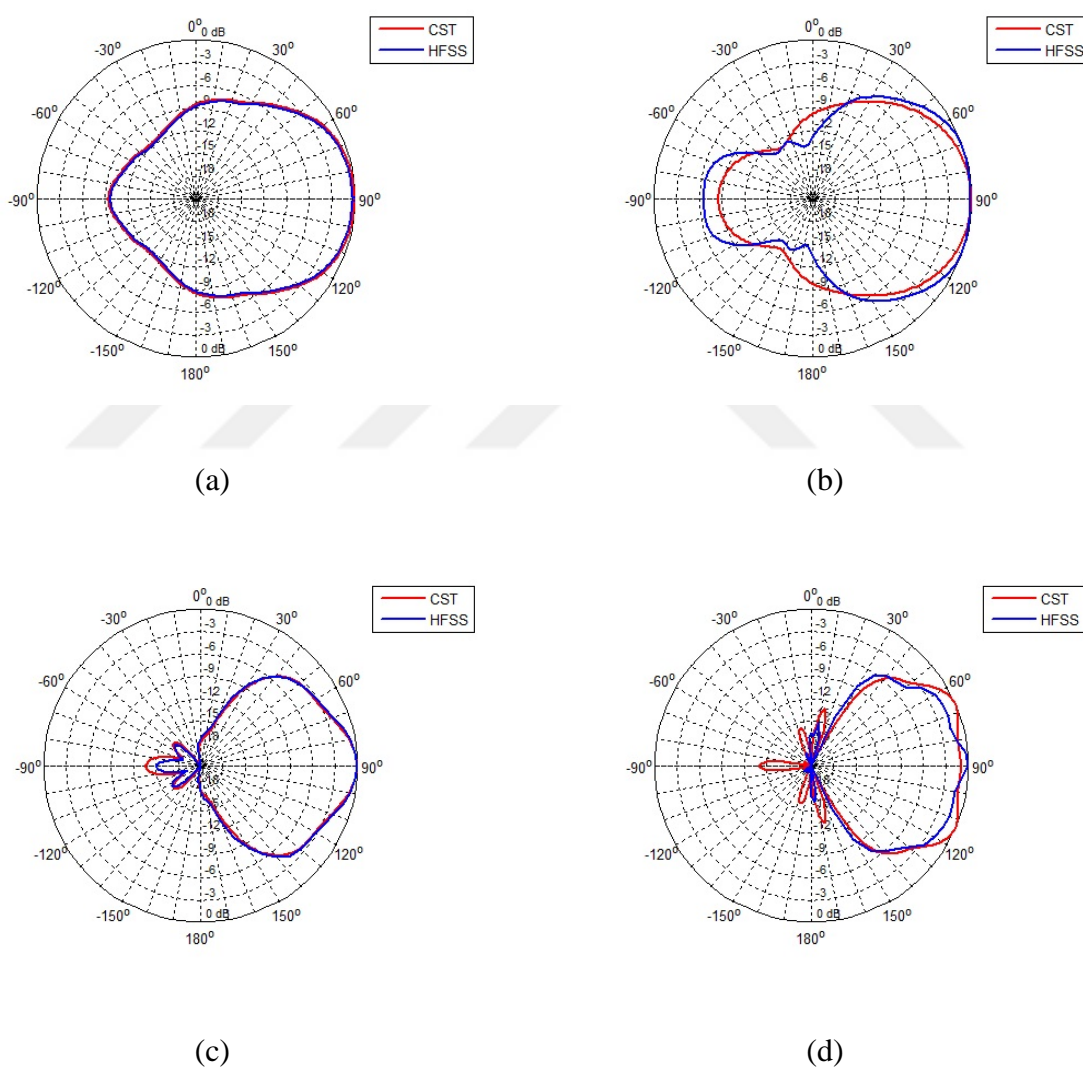
Figure 3.5 Directivity of the DREBT antenna at $\varphi = 90°$ for a) 500 MHz b) 1 GHz c) 2 GHz d) 3 GHz.

Directivity of the antenna is compared with electromagnetic simulation programs CST Microwave Studio and Ansoft HFSS and depicted at different frequencies in Fig. 3.5. It is noticeable to mention that the DREBT antenna directivity increases at higher frequencies. We depict the directivity to show that the amplitude of the received signal can be used in algorithm to obtain a better DF accuracy. The radiation efficiency at 500 MHz is about %97 while with the increase in frequency is reduces to %69 at 3 GHz. Actually such a decrease in realized gain do not have remarkable effect on the practical DF applications (Ozturk et al., 2015).

3.2.1.2 Loaded Bi-Conical Antenna

Loaded bi-conical antenna is developed for monitoring purposes. Monitoring antenna is needed because the directed antennas are used for direction finding. In practically, omni-directional antenna is needed to capture the unknown signal from all directions with the same amplitude (Ghosh et al., 2009). Length of the arm and loaded disc size are optimized with HFSS simulation program. Length of the arm is 25 cm where loaded disc radius is 5 cm with 1 cm port gap.

| (a) | (b) |
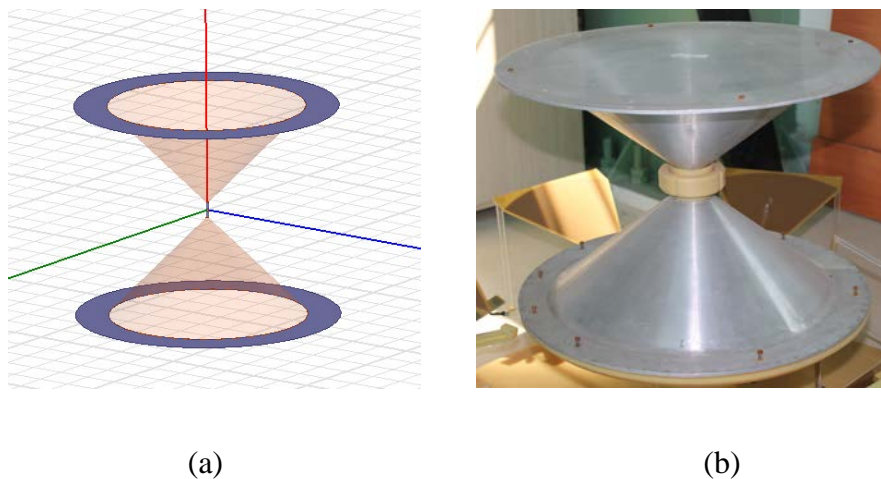
Figure 3.6 Loaded Bi-Conical Antenna a) Simulated antenna b) Realized antenna.

In Fig. 3.6 (a), simulated model of the loaded bi-conical antenna is seen where manufactured one is in Fig. 3.6 (b). Return loss is shown in Fig. 3.7. These values are not lower than -10 dB. However, return loss is satisfying its usage aim for receive purposes and with the aid of microwave amplifiers the received signals are sensible. Directivity of the antenna is simulated in both HFSS and CST, and the results are depicted in Fig. 3.7. The results are in good agreement. It's clear that antenna is omni-directional for all interested frequency range.
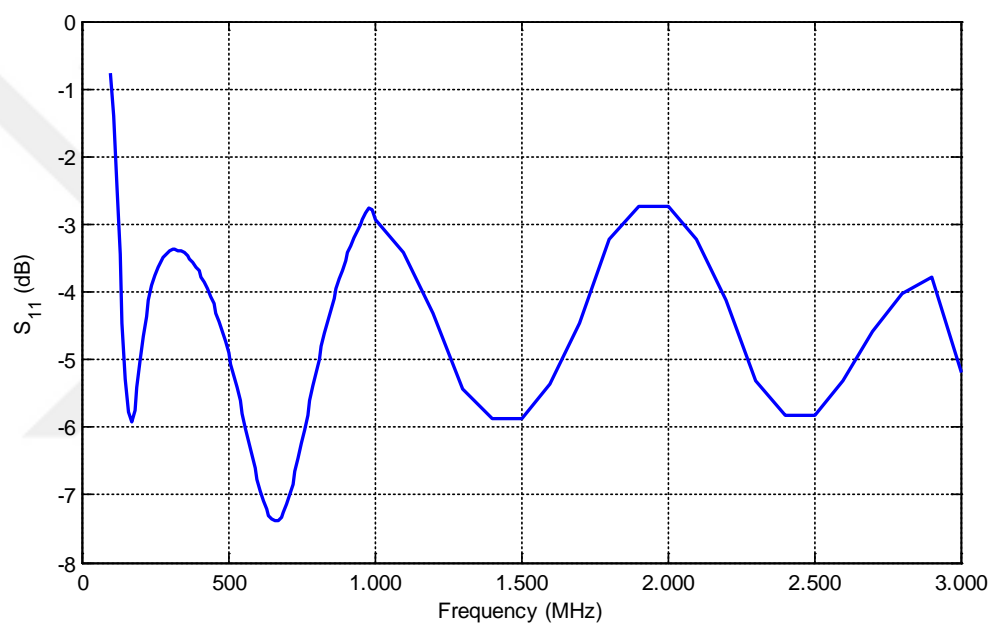
Figure 3.7 Return Loss of the Loaded Bi-Conical Antenna.

(a)

(b)

(c)

(d)
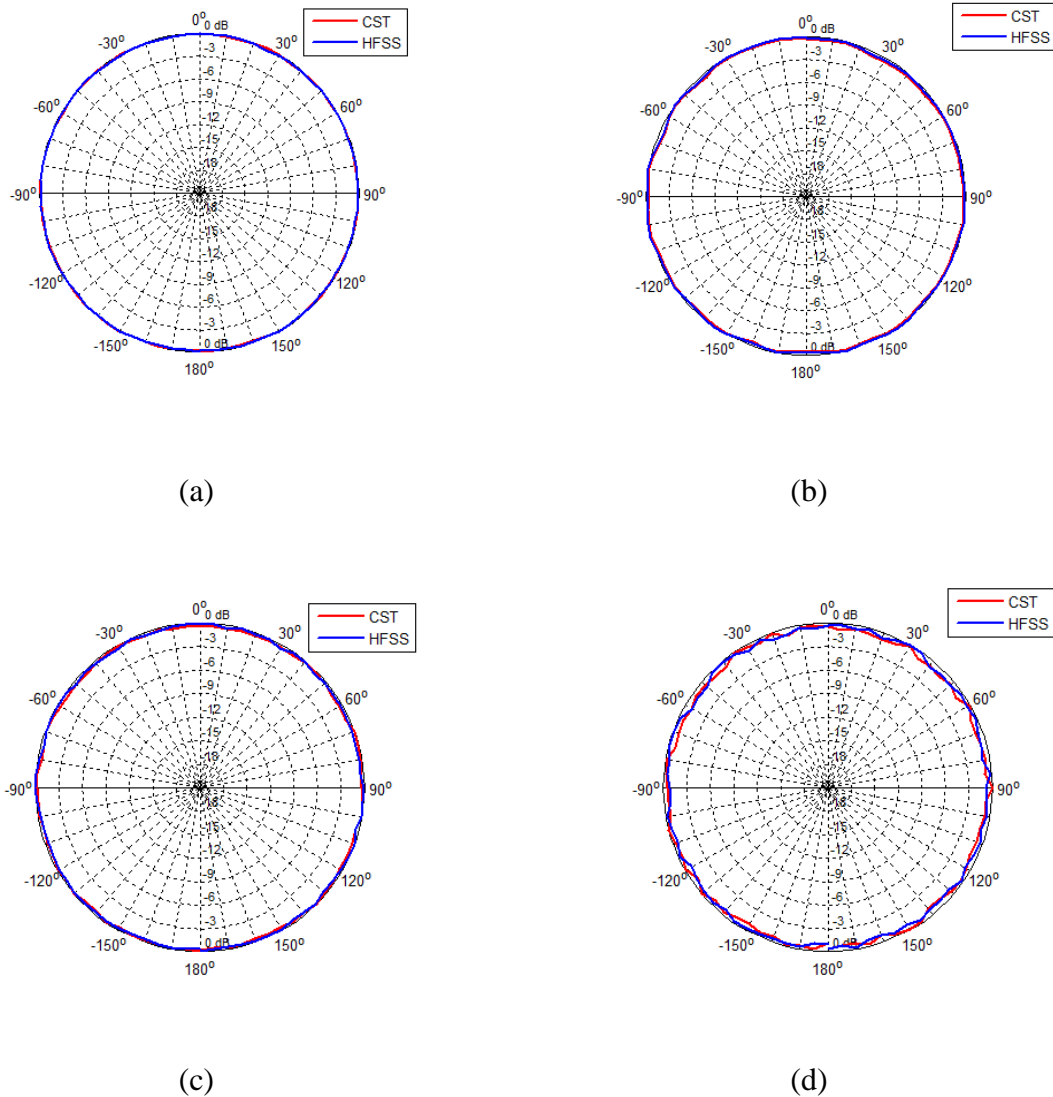
Figure 3.8 Directivity of the Loaded Bi-Conical Antenna at φ = 90° for a) 500 MHz b) 1 GHz c) 2 GHz d) 3 GHz.

3.2.2 Direction Finding Receivers and Other Components

The antenna array is the front part of the DF system that takes the electromagnetic waves from the air. RF signals should be decreased to an IF to be processed by the DF processor. This crucial process is done by the DF processors. The most important difference of the DF receivers from classical receivers is the use of the same frequency synthesizer in all DF receivers for the phase and amplitude matched conversion from RF to IF. In order to decrease the calculation time of the angle of arrival, the number of receivers should be increased up to the number of antennas in the antenna array. On the

other hand, increasing the number of DF receivers increases the power consumption proportionally and the cost of the hardware increases exponentially.

Two channel National Instrument receiver that is NI PXIe-1078 Chassis with NI PXIe-8106 Embedded Controller, NI PXIe-5601 RF Downconverter, NI PXIe-5622 16-bit IF Digitizer and NI PXI-5652 RF Signal Generator is used (see Fig. 3.9). Because of the number of used receiver channels, an RF switch which has nine inputs and two outputs is used.

Motor in Fig. 3.10 is used for rotating antenna array in azimuth axis. Measurement setup will discuss under chapter 4. Two different motor is used for indoor and outdoor purposes as seen in Fig. 3.10 (a) and (b). Motors have 1 degree of resolution.
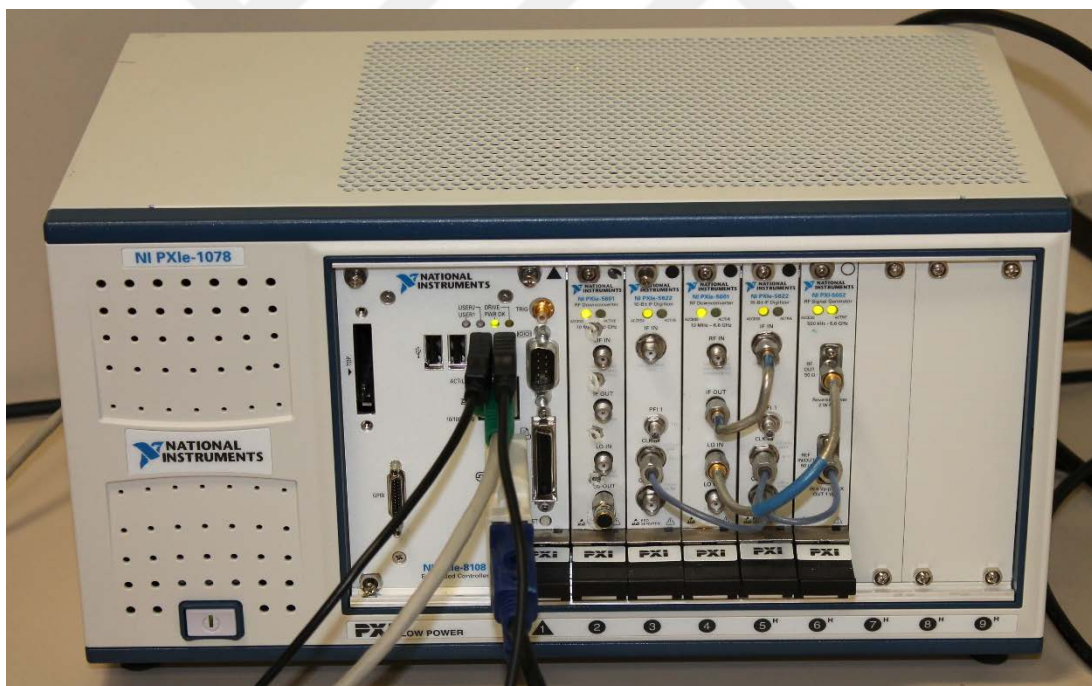
Figure 3.9 NI PXIe-1078 Chassis with NI PXIe-8106 Embedded Controller, NI PXIe-5601 RF Downconverter, NI PXIe-5622 16-bit IF Digitizer and NI PXI-5652 RF Signal Generator.

There is a need for a Global Positioning System (GPS) to help us to locate the vehicle position and also the direction of vehicle to estimate the target signal position. For that purpose the commercial GPS receiver from Trimble is used (see Fig. 3.11).

Uninterruptible Power Supply (UPS) and battery is also used in field tests.

(a)   (b)
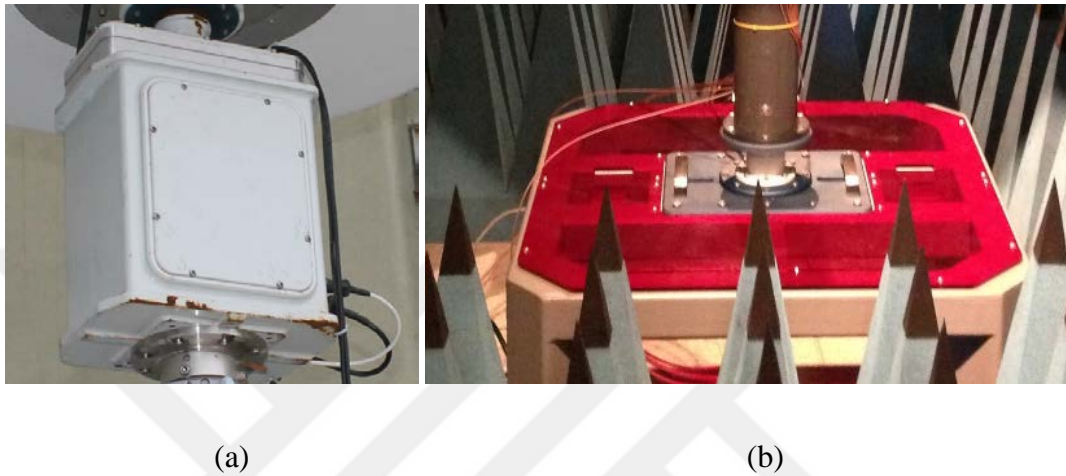
Figure 3.10 Motors (a) outdoor usage (b) indoor usage.

Figure 3.11 Trimble BX982 GPS Receiver.

3.3 SOFTWARE OF A DIRECTION FINDING SYSTEM

Software of designed DF system consist of;

1. Estimation algorithm
2. Triangulation algorithm
3. Mapping software

NI CVI programming tool is used to program the DF receiver for obtaining the signal and for further processing. Correlative interferometer algorithm is used as an estimation algorithm. Recursive estimation with extended Kalman filter is selected to triangulate the exact position of target signal. Finally, open source mapping program is used to show the results in the map with vehicle position.

3.3.1 Correlative Interferometer Algorithm

Once a signal has been received and detected it is passed to the signal processor. The signal processor analyzes properties of the signal to determine characteristics of the signal, such as phase, frequency, and amplitude. A wide variety of tools and techniques
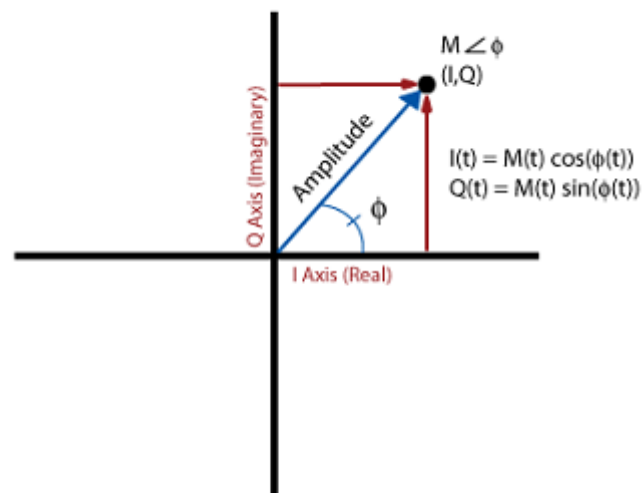
Figure 3.12 Polar and I-Q coordinates, where M is the magnitude of the wave, t is time, φ is the phase, I is the real component of the wave, and Q is the imaginary component.

have been developed to extract this information from received signals. Two common used techniques are in-phase and quadrature analysis by using of frequency domain analysis with Fourier transform (Poor, 1994).

In-phase and quadrature analysis (I-Q analysis) represents a real valued signal as a combination of real (I) and imaginary (Q) components. Having a signal split into real and imaginary parts reduces the complexity for determining the frequency and phase. The general function for a real valued sine wave is given by:

$$x(t) = Asin(2\pi ft + \delta) \tag{3.1}$$

where A is the amplitude, f is the frequency (Hz), and δ is the phase shift. In this form, the total instantaneous phase of the wave, $\Phi(t) = 2\pi ft + \delta$, depends on δ. In order to calculate Φ and A directly, the function must be altered. Using trigonometric identities Eq. (3.1) can be rewritten as:

$$x(t) = Asin(\delta)cos(2\pi ft) + Acos(\delta)\sin(2\pi ft) \tag{3.2}$$

$$= A_1 cos(2\pi ft) + A_2 \sin(2\pi ft)$$

where $A_1 = Asin(\delta)$ and $A_2 = Acos(\delta)$. The two components of the sinusoid are: the sine (in-phase) component, $I = A_2 \sin(2\pi ft)$, and cosine (quadrature) component, $Q = A_1 cos(2\pi ft)$. The I and Q components are a conversion of polar coordinates to the Cartesian plane as shown in Fig. 3.12. The relationship between I and Q allows for the calculation of instantaneous phase by taking the arctangent of I and Q components as shown in Eq. 3.3. The amplitude is calculated by using the Pythagorean Theorem as shown in Eq. 3.4:

$$\Phi = \tan^{-1}(Q/I) \tag{3.3}$$

$$A^2 = I^2 + Q^2 \tag{3.4}$$

Much like I-Q analysis, the Fourier transform represents the real signal as a combination of real and imaginary parts; however, the Fourier transform also changes the signal from the time domain to the frequency domain, showing which parts of the signal are present at each frequency. The Fourier transform is given by the equation:

$$X(\omega) = \int_{-\infty}^{\infty} x(t)e^{-j\omega t}dt \tag{3.5}$$

where $x(t)$ is the signal in the time domain, $X(\omega)$ is the signal in the frequency domain, t is the time, and ω is the frequency. The Fourier transform uses an integral across the entire time domain. The integral spans every point in time; however, in a digital system, data only exists for a time range and only at sampling intervals within that range. Therefore, digital systems use the discrete Fourier transform (DFT) which replaces the integral over all time with a sum of samples in a specified range. The DFT can be found by the equation:

$$X(k) = \sum_{n=0}^{N_0} x_n e^{-jk(\frac{2\pi}{N_0})n} \qquad (3.6)$$

where x_n is the nth sample of the signal in time domain, $X(k)$ is the kth sample of signal in frequency domain, and N_0 is the taken number of samples. The transformation expresses the waveform as a series of harmonics, each with a specific amplitude, frequency, and phase. By comparing the magnitude of the different frequency components, the frequency or frequencies of the signal are determined. When the strength of a signal is large compared to the noise present, the frequency components of the signal have a higher magnitude than the frequency components of the noise.

For practical applications, the DFT can be inconvenient to use because the number of computations required is O(N^2) where N is the number of samples used in the calculation. The accuracy of the DFT increases with the number of terms used because it becomes a closer approximation of the regular Fourier transform. Due to the potentially large number of calculations required for the DFT, many systems use fast Fourier transform (FFT) algorithms which take advantage of the linearity of the DFT to perform the DFT on a number of shorter signals and then combine the results. FFT algorithms reduce the number of computations needed to O($N\log_2 N$) in cases where N is a power of 2. These signal processing techniques simplify the process of extracting phase and frequency information that direction finding systems can use to calculate the AoA of a signal (Friedlander and Ksienski, 1991).

Correlative interferometer is a technique that uses phase difference between captured incident signals from neighboring antennas to compute AoA. The real condition of the travelling signal from transmitter to antennas is shown in Fig. 3.13 (a). If the transmitter is sufficiently far away, we can assume that d1 and d2 are parallel to each other as shown in Fig 3.13 (b).
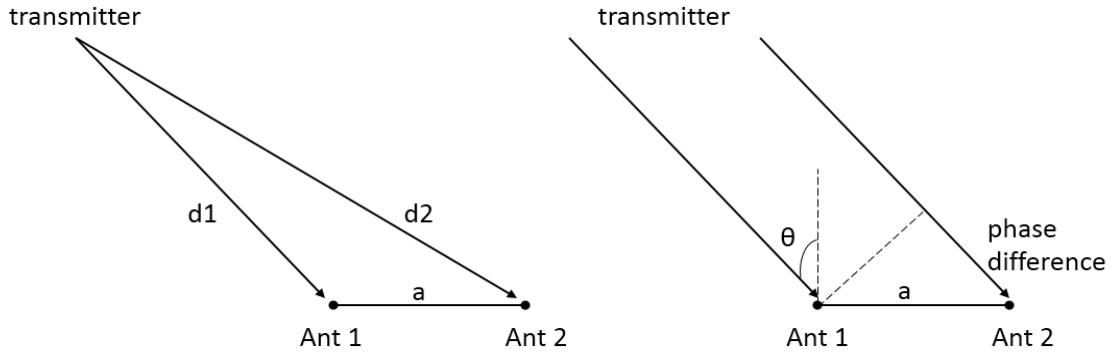
Figure 3.13 Phase difference, ΔΦ, is mapped from AoA for antenna separation a and incident wavelength λ.

Signal received at antenna 1 travels an additional distance $(a \times sin\theta)$ with respect to antenna 2. The time to travel this distance between antenna 1 and antenna 2 creates a phase difference. The voltage received by antenna 1 is

$$V_1 = Ve^{-j\omega t} \tag{3.7}$$

where V is the initial transmitted signal amplitude. Signal travels an additional distance $(a \times sin\theta)$ to reach antenna 2, thus the voltage received by antenna 2 can be expressed as:

$$V_2 = Ve^{j\omega t + \frac{2\pi}{\lambda} a sin\theta} \tag{3.8}$$

where a equals to the antenna aperture and $2\pi/\lambda$ is the free space propagation constant. Subtracting V_2 from V_1 and taking to the natural logarithm of both sides in order to obtain voltage differences between antennas yields:

$$\ln V_2 - \ln V_1 = \ln \frac{V_2}{V_1} = \frac{2\pi}{\lambda} a sin\theta \tag{3.9}$$

Initial transmitted signal amplitude V is used in both Eq. 3.7 and Eq. 3.8. So it is eliminated in Eq. 3.9. Thus, it represents $\Delta\Phi$, which is the phase difference between antenna 1 and antenna 2:

$$\Delta\Phi = \frac{2\pi}{\lambda} a sin\theta \tag{3.10}$$

The AoA, θ, can be calculated from Eq. 3.10 as:

$$\theta = \sin^{-1}(\Delta\Phi\lambda/2\pi a) \tag{3.11}$$

The distance between receiving antennas, a, in DF antenna array must be chosen carefully. For an unambiguous AoA estimation, a should be smaller than the half wavelength of the highest frequency of incident wave if not multiple AoAs can produce the same phase difference in multiples of 2π. On the other hand, smaller antenna distances, a, decreases the phase resolution for the lower frequencies and results in increased AoA errors. Fig. 3.14 shows the calculated phase differences between antenna pairs 2-1, 3-2, 4-3 and 1-4 after adding proper offsets to prevent the phase ambiguities.

The angle of arrival is computed using correlative interferometer algorithm in computation process as shown in Fig. 3.15. First, the phase difference between signals at the antennas is calculated from obtained digitized signal. Then, the phase difference vector is compared with those obtained for a DF system of known configuration at a given wave angle and given frequency (Johnson 1982).
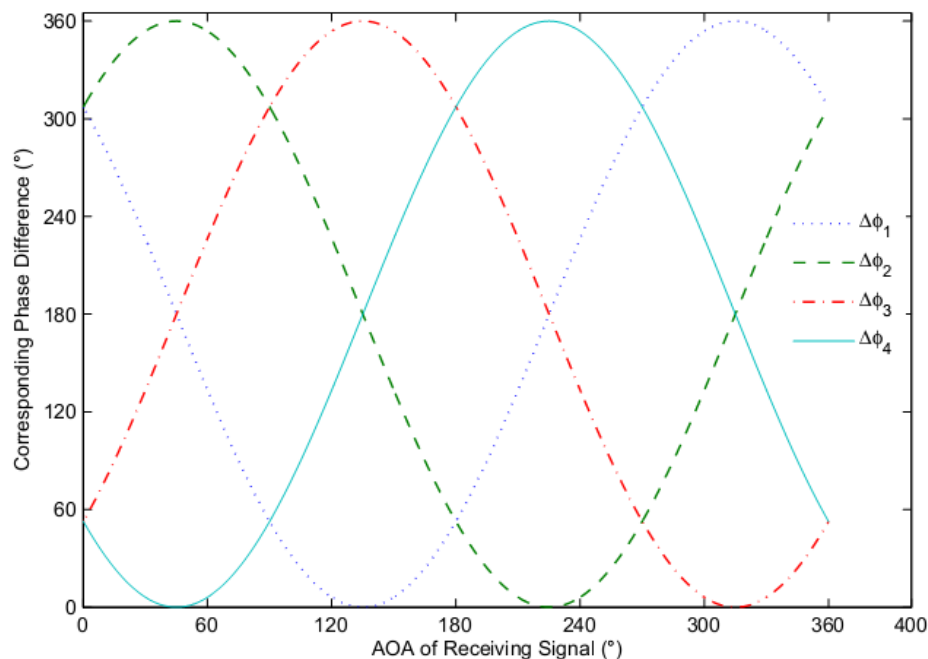
Figure 3.14 Calculated Phase Differences between Antennas 2-1, 3-2, 4-3 and 1-4 for a=λ/2.
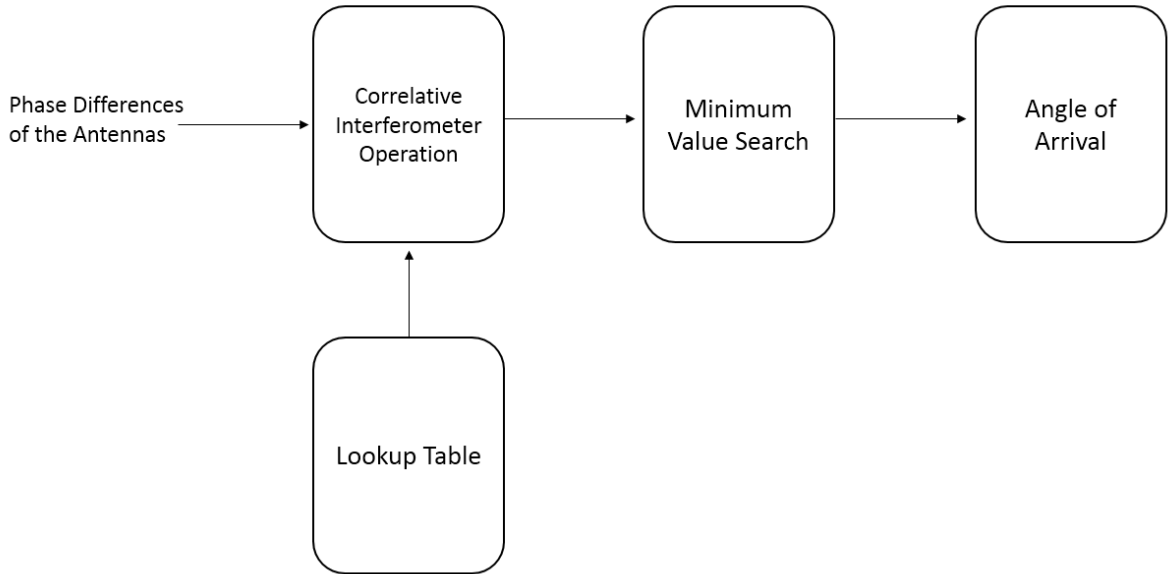
Figure 3.15 Correlative Interferometer Blog Diagram.

In addition to the correlative interferometer technique, amplitude of the incident signal is considered to calculate AoA. Firstly, the direction of the maximum amplitude value of the signal that occurs at the antennas is found. Then, correlative interferometer operation is taken around at the $\pm\,25°$ of the maximum amplitude. Afterwards, k-means clustering, well defined in the literature, is used to minimizing the error.

While speaking of DF accuracy, Root-Mean-Square (RMS) error is one of the tools that show us the DF system goodness. RMS of the AoA of DF system is defined as

$$RMS_{err} = \sqrt{\frac{\sum_{i=1}^{n}(e_i - e_A)^2}{n}} \qquad\qquad (3.12)$$

where e_i is the error at the ith azimuth angle, n the number of azimuth angles and $e_A = \frac{\sum_{i=1}^{n} e_i}{n}$ is the normalized azimuth angel (Balanis, 2005).

For a 300 number of data, the calculated AoA's with correlative interferometer results are shown in Fig 3.16. Where high errors can be eliminated by using of k-means clustering. Example is given for four frequencies (350, 750, 1500 and 2500 MHz) though the results for other frequencies are similar.
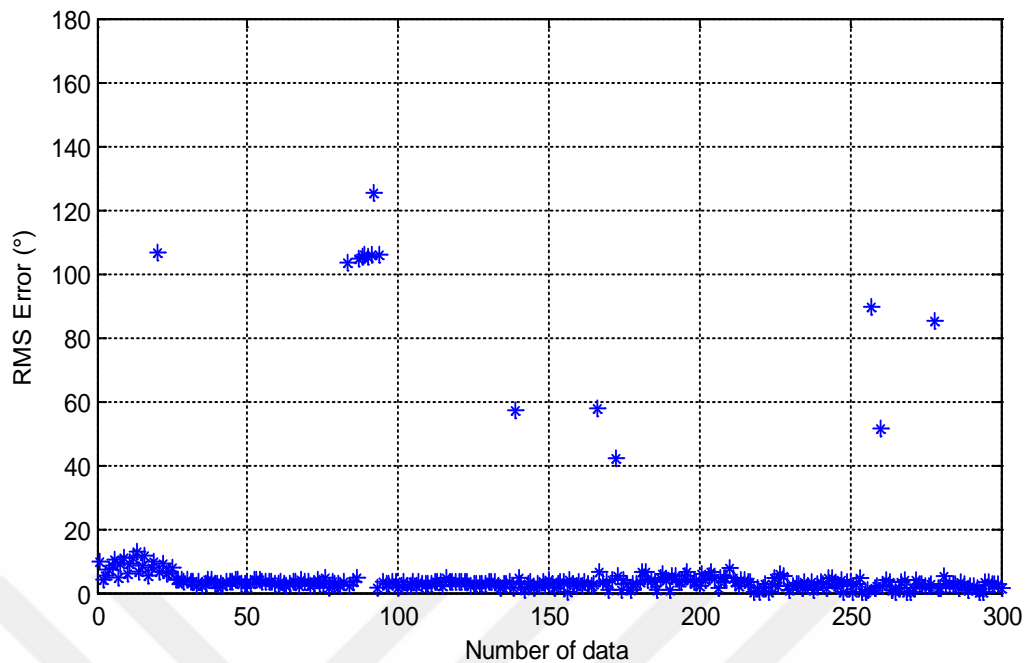
(a)
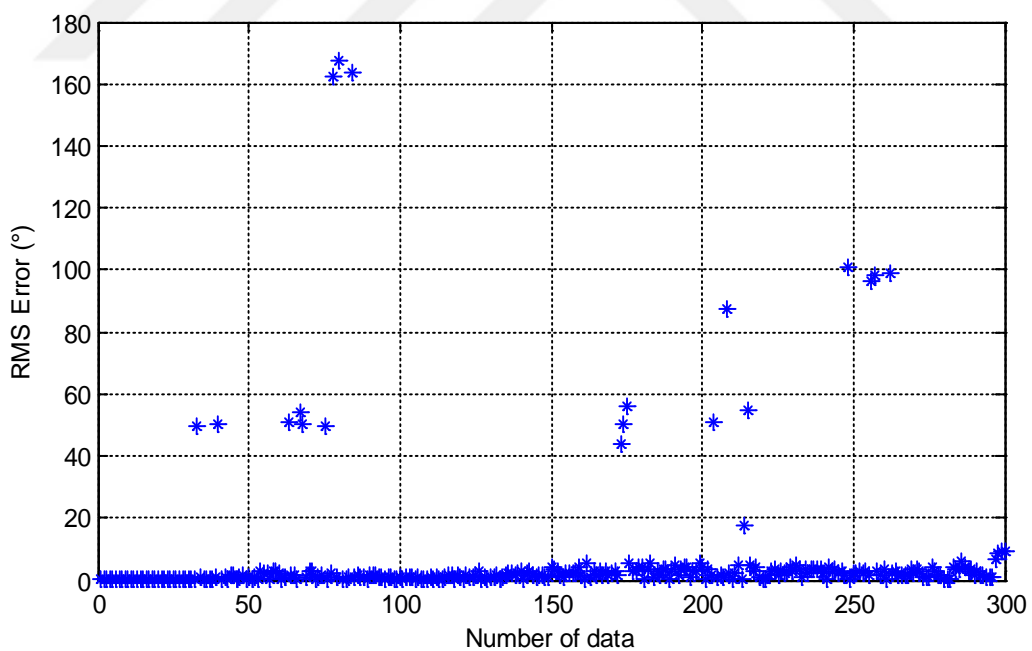
(b)

Figure 3.16 Example of calculated AoA's results at a) 350 MHz b) 750 MHz c) 1500 MHz d) 2500 MHz.
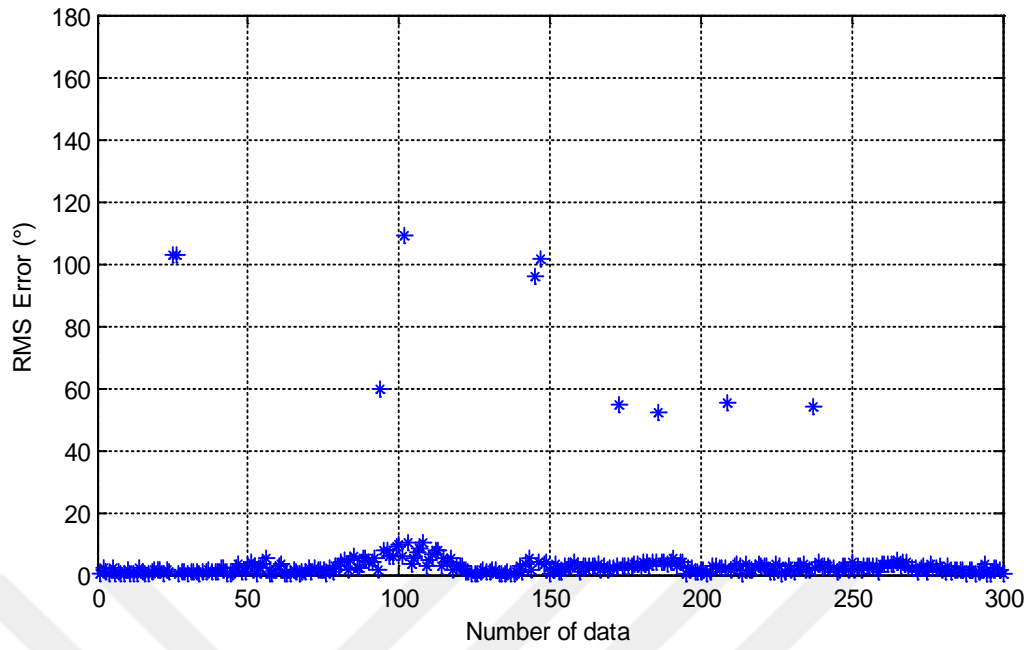
(c)
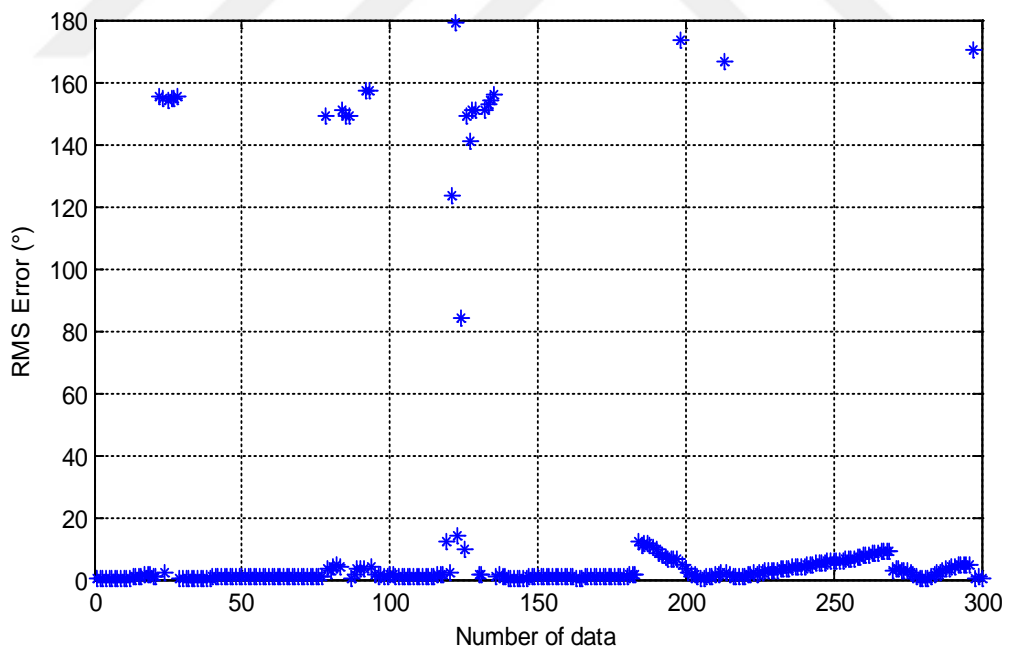
(d)

Figure 3.16 Example of calculated AoA's results at a) 350 MHz b) 750 MHz c) 1500 MHz d) 2500 MHz.

3.2.2. Euclidean Distance

We use Euclidean distances of measurement data to form a lookup table for the correlation method. The minimum Euclidean distance implies the maximum correlation. Distance, d, for N dimensional vectors **x** and **y** can be calculated by

$$d = \sqrt{\sum_{i=1}^{N}(x_i - y_i)^2} \tag{3.13}$$

Fig. 3.17 shows Euclidean distances of measured data with an AoA of 50° with added noise to signal with 0 dB signal to noise ratio (SNR).
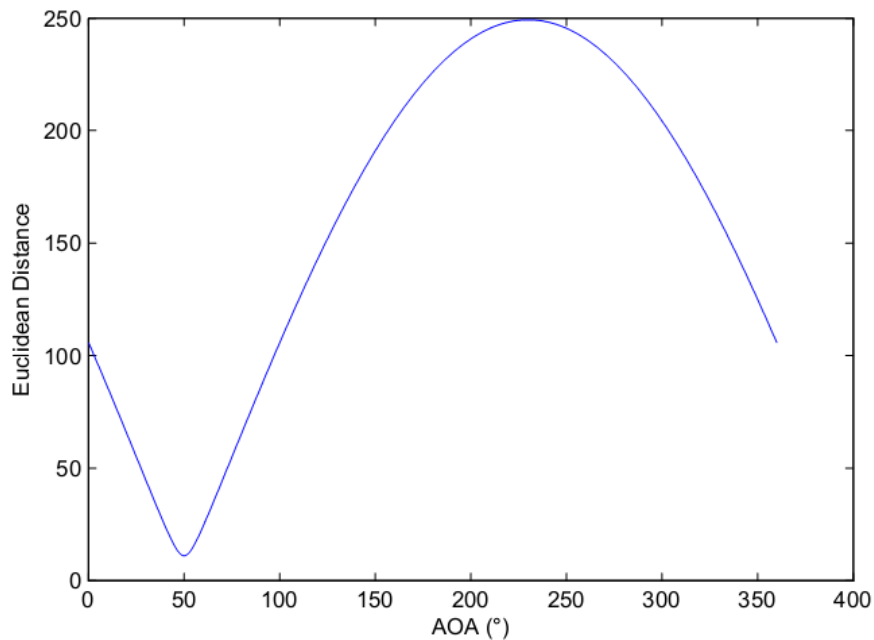
Figure 3.17 Euclidean distances of an AoA of 50° with 0 dB SNR.

3.2.3 Triangulation Algorithms

Once a signal has been received and detected it can be localized by triangulation methods. To use the triangulation methods, at least two or more different DF system is needed as depicted in Fig.3.18. Many triangulation methods are described in literature. Least squares, pseudo-linear, weighted instrumental variables and maximum likelihood estimation methods are well known triangulation methods (Zhou, 2005).

Coordinate system is depicted in Fig.3.15, where $\mathbf{r}_k$ is the DF system position while P is the target signal position. Target position with respect to DF system at k^{th} measurement will be

$$\mathbf{s}_k = |\mathbf{s}_k| \begin{bmatrix} \cos\phi_k \cos\theta_k \\ \cos\phi_k \sin\theta_k \\ \sin\phi_k \end{bmatrix} \qquad (3.14)$$

where ϕ_k is the elevation angle and θ_k is the azimuth angle as seen at Fig. 3.19.
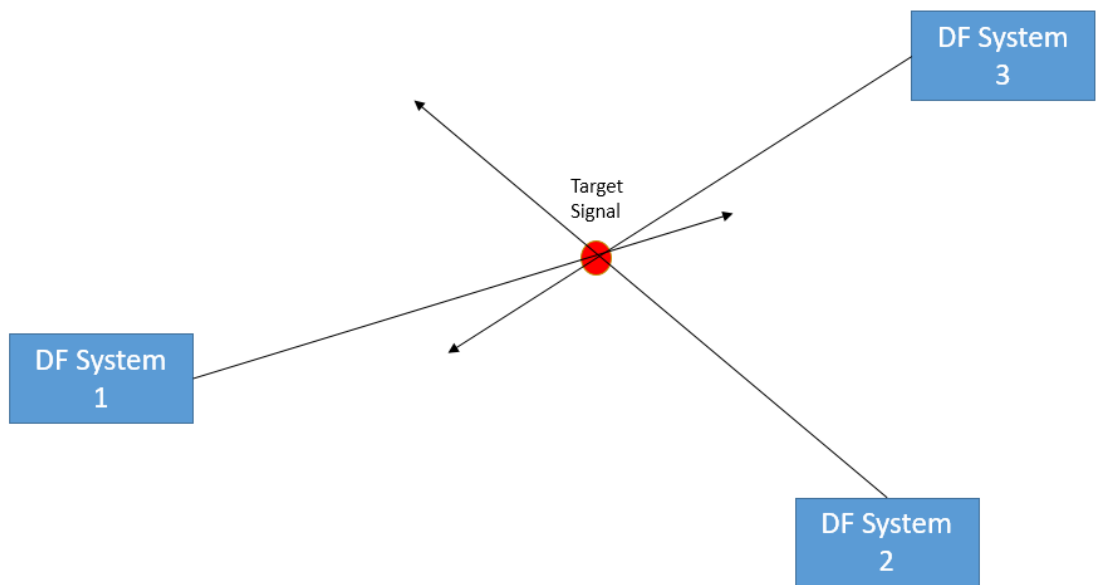
Figure 3.18 Sample Sequence of DF Systems for Triangulation Methods.

$$\theta_k = \tan^{-1}\left(\frac{y_P - y_k}{x_P - x_k}\right) \qquad (3.15)$$

$$\phi_k = \tan^{-1}\left(\frac{z_P - z_k}{\sqrt{(x_P - x_k)^2 - (y_P - y_k)^2}}\right) \qquad (3.16)$$
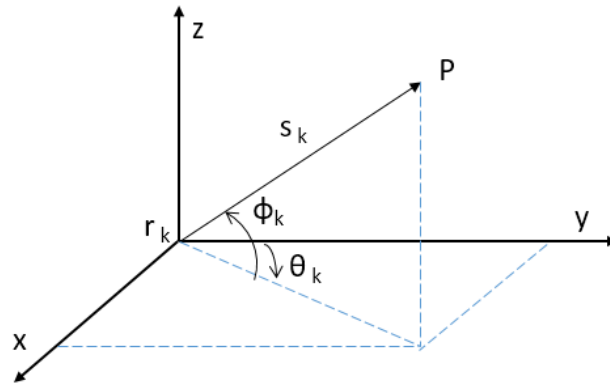
Figure 3.19 Coordinate System and Positioning.

P, the target signal position can be defined as

$$\mathbf{P} = \mathbf{r}_k + \mathbf{s}_k \tag{3.17}$$

With defined estimation methods, position of the target, $\mathbf{P}$ will be found.

3.2.3.1. Least-Squares Estimation Method

In LSE method (Wu, 1991), vector $\mathbf{A}$ will be defined rectangular to $\mathbf{s}_k$ as

$$\mathbf{A} = \begin{bmatrix} \cos\left(\phi_k + \dfrac{\pi}{2}\right)\cos\theta_k \\ \cos\left(\phi_k + \dfrac{\pi}{2}\right)\sin\theta_k \\ \sin\left(\phi_k + \dfrac{\pi}{2}\right) \end{bmatrix} = \begin{bmatrix} -\sin\phi_k\cos\theta_k \\ -\sin\phi_k\sin\theta_k \\ \cos\phi_k \end{bmatrix} \tag{3.18}$$

If Eq. 3.16 is multiplied with transpose of vector $\mathbf{A}$, Eq. 3.18 will be simplified as

$$\mathbf{A}^T\mathbf{P} = \mathbf{A}^T\mathbf{r}_k + \mathbf{A}^T\mathbf{s}_k \tag{3.19}$$

$$\mathbf{P} = \left(\mathbf{A}^T\mathbf{A}\right)^{-1}\mathbf{b} \tag{3.20}$$

Least-Squares Estimation (LSE) Procedure:

- AoA is computed from the unknown signal at each measured data with a DF algorithm.

- Matrix **A** and vector **b** is obtained as referred to Eq. 3.18-19 with using the obtained AoA measurements and DF system positions.
- Target position **P** is obtained by using the equation given at Eq. 3.20.

3.2.3.2. Pseudo-Linear Estimation Method

In this method, position is firstly analyzed at azimuth angles to estimate x_P and y_P. Then, using elevation angles, z_P is estimated. Eq. 3.15 can be rewritten as

$$\tan\theta_k = \frac{y_P - y_k}{x_P - x_k} \tag{3.21}$$

$$\frac{\sin\theta_k}{\cos\theta_k} = \frac{y_P - y_k}{x_P - x_k} \tag{3.22}$$

$$\sin\theta_k\left(x_P - x_k\right) = \cos\theta_k\left(y_P - y_k\right) \tag{3.23}$$

$$x_P\sin\theta_k - x_k\sin\theta_k = y_P\cos\theta_k - y_k\cos\theta_k \tag{3.24}$$

$$x_P\sin\theta_k - y_P\cos\theta_k = x_k\sin\theta_k - y_k\cos\theta_k \tag{3.25}$$

Eq. 3.24 can be written for all *N* measurements and can be expressed as

$$\underbrace{\begin{bmatrix} \sin\theta_1 & -\cos\theta_1 \\ \vdots & \vdots \\ \sin\theta_N & -\cos\theta_N \end{bmatrix}}_{\mathbf{A}_1}\underbrace{\begin{bmatrix} x_P \\ y_P \end{bmatrix}}_{\mathbf{P}_{xy}} = \underbrace{\begin{bmatrix} \sin\theta_1 x_1 - \cos\theta_1 y_1 \\ \vdots \\ \sin\theta_N x_N - \cos\theta_N y_N \end{bmatrix}}_{\mathbf{b}_1} \tag{3.26}$$

x_P and y_P coordinates of the target is estimated by

$$\mathbf{P}_{xy} = \left(\mathbf{A}_1^T\mathbf{A}_1\right)^{-1}\mathbf{A}_1^T\mathbf{b}_1 \tag{3.27}$$

Then, z_P coordinate of the target is estimated by using Eq. 3.16 with found values of x_P and y_P. For *N* measurements the following formula is used

$$z_P = \frac{1}{N}\sum_{k=1}^{N}\left(z_k + \sqrt{\left(x_P - x_k\right)^2 - \left(y_P - y_k\right)^2}\tan\phi_k\right) \tag{3.28}$$

Pseudo-Linear Estimation (PLE) Procedure:

- AoA of the unknown signal is computed at each measured data with a DF algorithm.

- Matrix $\mathbf{A}_1$ and vector $\mathbf{b}_1$ is obtained as referred to Eq. 3.26 by using the estimated azimuth measurements and DF system positions.

- x and y coordinates of the unknown signal $\mathbf{P}_{xy}$ is estimated by using the equation in Eq. 3.27.

- z coordinate of the unknown signal is obtained by using $\mathbf{P}_{xy}$, estimated elevation measurements and DF system positions in Eq. 3.28.

3.2.3.3. Weighted Instrumental Variables Estimation Method

Since the measurement matrix $\mathbf{A}_1$ is correlated with noise, the PLE is not consistent. As N goes to infinity, $\mathbf{P}_{xy}$ does not converge to true location vector. Weighted Instrumental Variables Estimation (Mueller et al., 2006) is used to solve this problem.

Instrumental variable matrix $\mathbf{G}_1$ that is uncorrelated with noise, is multiplied in Eq. 3.26

$$\left(\mathbf{G}_1^T \mathbf{A}_1\right)\mathbf{P}_{xy} = \mathbf{G}_1^T \mathbf{b}_1 \tag{3.29}$$

where $\mathbf{G}_1$ is constructed by using estimated azimuth angles:

$$\mathbf{G}_1 = \begin{bmatrix} \sin\theta_1 & -\cos\theta_1 \\ \vdots & \vdots \\ \sin\theta_N & -\cos\theta_N \end{bmatrix} \tag{3.30}$$

Estimated target is:

$$\mathbf{P}_{xy} = \left(\mathbf{G}_1^T \mathbf{A}_1\right)^{-1} \mathbf{G}_1^T \mathbf{b}_1 \tag{3.31}$$

Instrumental variable matrix is uncorrelated with the noise. The coherence of the estimate is determined and the estimator is converted to asymptotically unbiased by using an instrumental variable matrix. Coordinate of the target, z_P, is estimated by Eq. 3.28 with new values of x_P and y_P as

$$z_P = \frac{1}{N}\sum_{k=1}^{N}\left(z_k + \sqrt{\left(x_{P,WIVE} - x_k\right)^2 - \left(y_{P,WIVE} - y_k\right)^2}\,\tan\phi_k\right) \tag{3.32}$$

Weighted Instrumental Variables Estimation (WIVE) Procedure:

- AoA of the unknown signal is computed at each measured data with a DF algorithm.

- Azimuth angles are calculated by using the $\mathbf{P}_{xy}$ estimation that is obtained PLE in Eq. 3.15.

- $\mathbf{G}_1$ is estimated with using the obtained azimuth angles in Step 2 with Eq. 3.30.

- Distance between unknown signal and DF system positions is estimated with using the estimate that is calculated with PLE.

- x and y coordinates of the unknown signal $\mathbf{P}_{xy,}$ is calculated by using the equation in Eq. 3.31.

- z coordinate of the unknown signal is estimated with using the equation in Eq. 3.32.

3.2.3.4. Maximum Likelihood Estimation Method

The Maximum Likelihood Estimation (MLE) is acquired from the highest of the joint probability density function of the measured data. Noise is assumed that is zero mean Gaussian. And, MLE of the unknown signal position can be written as

$$\mathbf{P}_{MLE} = \arg\min J_{MLE}(\mathbf{P}) \tag{3.33}$$

where the MLE cost function is given by

$$J_{MLE}(\mathbf{P}) = \mathbf{e}^T(\mathbf{P})\mathbf{K}^{-1}\mathbf{e}(\mathbf{P}) \tag{3.34}$$

$\mathbf{K}$ is the *2Nx2N* covariance matrix of the noise where $\mathbf{e}(\mathbf{P})$ is the *2Nx1* error vector that are written as

$$\mathbf{K} = diag\left\{\sigma^2_{\theta_1},\sigma^2_{\theta_2},\cdots,\sigma^2_{\theta_N},\sigma^2_{\phi_1},\sigma^2_{\phi_2},\cdots,\sigma^2_{\phi_N}\right\} \tag{3.35}$$

$$\mathbf{e}(\mathbf{P}) = \left[\theta_1 - \theta_1(\mathbf{P}),\cdots,\theta_N - \theta_N(\mathbf{P}),\phi_1 - \phi_1(\mathbf{P}),\cdots,\phi_N - \phi_N(\mathbf{P})\right] \tag{3.36}$$

It's obvious that MLE does not own a closed form solution. The unknown signal position is found with a search algorithm which gets the lowest cost. A batch iterative minimization technique is used for this purpose. The method is as follows

$$\mathbf{P}_{i+1} = \mathbf{P}_i - \left(\mathbf{J}_i^T\mathbf{K}^{-1}\mathbf{J}_i\right)^{-1}\mathbf{J}_i^T\mathbf{K}^{-1}\mathbf{e}(\mathbf{P}_i) \quad \text{for } i = 0,1,\cdots,N_{iteration} \tag{3.37}$$

where $\mathbf{J}_i$ is the *2Nx3* Jacobian matrix that is written as

$$\mathbf{J}_i = \begin{bmatrix} \dfrac{-(y_p - y_1)}{(x_p - x_1)^2 \left(\dfrac{(y_p - y_1)^2}{(x_p - x_1)^2} + 1 \right)} & \dfrac{1}{(x_p - x_1)^2 \left(\dfrac{(y_p - y_1)^2}{(x_p - x_1)^2} + 1 \right)} & 0 \\[2em] \vdots & \vdots & \vdots \\[1em] \dfrac{-(y_p - y_N)}{(x_p - x_N)^2 \left(\dfrac{(y_p - y_N)^2}{(x_p - x_N)^2} + 1 \right)} & \dfrac{1}{(x_p - x_N)^2 \left(\dfrac{(y_p - y_N)^2}{(x_p - x_N)^2} + 1 \right)} & 0 \\[2em] \dfrac{-(x_p - x_1)(z_p - z_1)}{\|p - r_1\|^2 \sqrt{(x_p - x_1)^2 + (y_p - y_1)^2}} & \dfrac{-(y_p - y_1)(z_p - z_1)}{\|p - r_1\|^2 \sqrt{(x_p - x_1)^2 + (y_p - y_1)^2}} & \dfrac{\sqrt{(x_p - x_1)^2 + (y_p - y_1)^2}}{\|p - r_1\|^2} \\[2em] \vdots & \vdots & \vdots \\[1em] \dfrac{-(x_p - x_N)(z_p - z_N)}{\|p - r_N\|^2 \sqrt{(x_p - x_N)^2 + (y_p - y_N)^2}} & \dfrac{-(y_p - y_N)(z_p - z_N)}{\|p - r_N\|^2 \sqrt{(x_p - x_N)^2 + (y_p - y_N)^2}} & \dfrac{\sqrt{(x_p - x_N)^2 + (y_p - y_N)^2}}{\|p - r_N\|^2} \end{bmatrix}_{P = P_i} \quad (3.38)$$

The initial estimate is necessary in the MLE method. To determine the initial estimation the methods explained before can be used. Jacobian matrix is assessed. After that, the estimate is updated considering to Eq. 3.37. This algorithm is running for a described iteration number or up to the norm of the position update if it is smaller than an adequate lower number. Selection of the initial estimate is an important part of the MLE method since cost function can diverge if the initial estimate is not close sufficiently to the unknown signal position.

Maximum Likelihood Estimation (MLE) Procedure:

- AoA of the unknown signal is computed at each measured data with a DF algorithm.
- Covariance matrix **K** is determined as described in Eq. 3.35.
- Error vector is determined with an initial unknown signal position that is described in Eq. 3.36.
- Jacobian matrix is calculated for the initial estimate with Eq. 3.38.
- Search algorithm that updates unknown signal position is running to determine at each step like at Eq. 3.37.
- While the defined update criterions are met, the search algorithm is finished.

3.2.3.5. Extended Kalman Filter

Various localization algorithms are introduced in previous sections. AoAs are used all at once to provide the unknown signal position in these methods. In particular

cases, if the location estimation is updated meantime the new data are collected, recursive location estimation may be chosen. In cases, there may not have sufficient space to store all measured positions where storage capacity is limited in the DF systems. Besides, the calculation capacity of the DF system can be restrictive. On the other hand, a recursive estimation only stores the position estimate and the new measured data. Firstly, a few measurements are taken. Then, a position estimate is determined that will be distant from the exact position. Finally, a new position estimate is determined with both the new measurement and predetermined position. DF systems do not need to store previous measurements. Kalman filter (KF) is used to solve this problem (Krim and Viberg, 1996).

When the system model is linear, KF is the optimal solution. But, the real life systems generally are nonlinear. To solve this problem, nonlinear system is linearized with assumptions. After, KF algorithm is used that is called the Extended Kalman Filter (EKF). Equations for EKF are written as:

$$x_{k+1} = f_k\left(x_k\right) \tag{3.39}$$

$$y_k = h_k\left(x_k\right) \tag{3.40}$$

where $f_k\left(\cdot\right)$ is the system model and $h_k\left(\cdot\right)$ is the measurement model.

In localization problem x_k is the unknown signal position for the kth time instant and y_k is the measurements that respectively are azimuth and elevation angles. Since the unknown signal is stationary the following equation holds:

$$x_{k+1} = x_k \tag{3.41}$$

The linearization process is only used for the measurement model while the state model is linear. The predicted state $x_{k+1|k}$ is used to linearize measurement relation.

$$y_{k+1} = h_{k+1}\left(x_{k+1|k}\right) + H_{k+1}\left(x_{k+1} - x_{k+1|k}\right) \tag{3.42}$$

$$H_{k+1} = \left(\nabla_{x_{k+1}} h_{k+1}^T\left(x_{k+1}\right)\right)^T \Bigg|_{x_{k+1}=x_{k+1|k}} \tag{3.43}$$

The state variables are coordinates of the unknown signal positions. Calculation of the gradient of the measurements vector with respect to state variables is done for the

linearization of the measurement model. The calculation of H_k matrix is same as the Jacobian matrix in MLE that is given previously.

3.2.4 User Interface

User interface is designed with NI CVI software. A sample power spectrum is shown in Fig. 3.20. AoA of the selected frequency at the power spectrum is shown in Fig. 3.21 with respect to vehicle direction. Also, dial format of the AoA is seen in Fig. 3.22.

Open source mapping software is used as seen in Fig. 3.23-24. In these figures, red point is target signal while start points of the arrows are the DF system positions. After applying triangulation algorithm target signal is found at the inside a narrow area which is shown in Fig. 3.24.
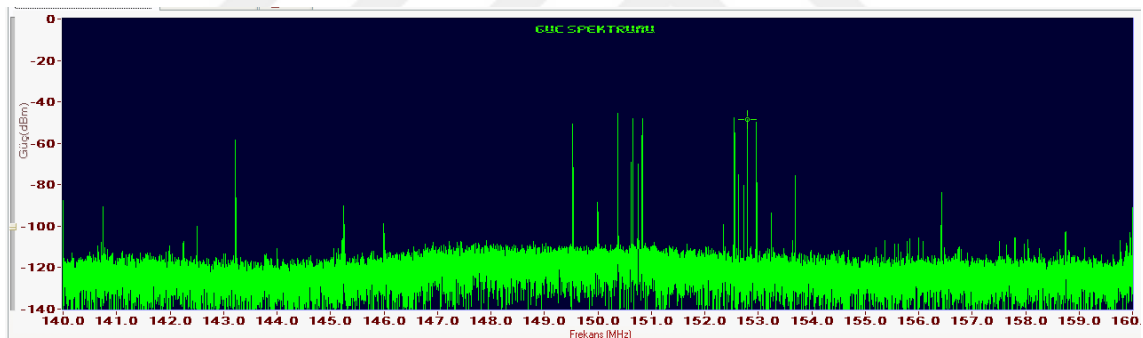
Figure 3.20 A sample power Spectrum of the User Interface.

Figure 3.21 AoA part of the User Interface.
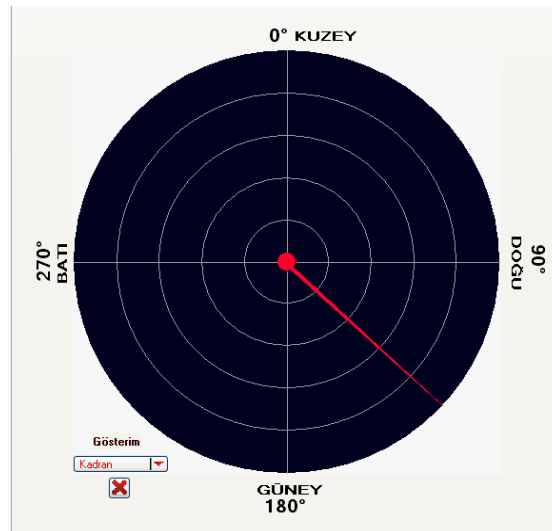
Figure 3.22 Dial format of the AoA at the User Interface.

Figure 3.23 Map Software with AoA's From Different Positions.
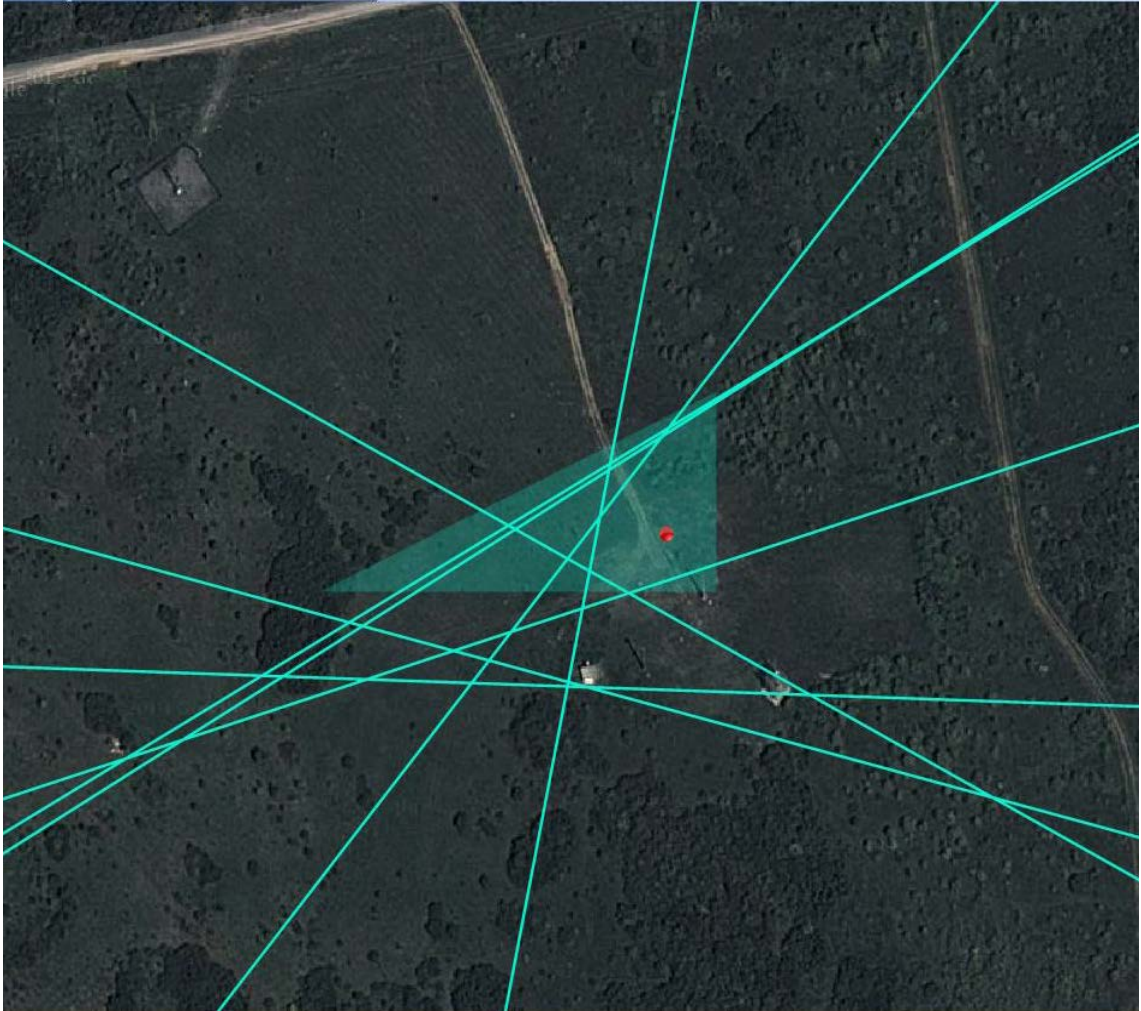
Figure 3.24 Triangulation of The Target Signal.

CHAPTER 4

EXPERIMENTAL VALIDATION OF THE DEVELOPED DIRECTION FINDING SYSTEM

4.1 INDOOR TEST RESULTS

Both the developed single antenna and the whole DF system has to be verified with measurements. To that end indoor measurements are conducted in an anechoic chamber. Firstly, the developed single DF antenna element is measured followed by the test of the whole DF system in a controlled environment. DREBT antenna that is introduced in Chapter 3 is used as a single DF antenna array element while loaded bi-conical antenna is used for monitoring purposes.

4.1.1 Single Direction Finding Antenna Measurement

In order to make the antenna array suitable for a vehicle mounted system with wideband frequency coverage, we proposed a DREBT antenna. The choice for a rounded edge design of the bow-tie radiator is based on our previous study which performs better for a wideband DF application. The DREBT antenna has two identical arms that look like a bow-tie antenna with rounded edge bended with a certain angle for directional propagation. The simulated and realized antenna is depicted in Fig. 4.1.

Due to simple production process and light weight issues the DREBT antenna is printed on FR4 substrate ($\varepsilon_r = 4.4$, thickness = 1.6 mm). During the modelling several parameter sweeps have been performed such as the length of the arm, flare angle of the arm and the number of antennas in DF antenna array in order to obtain the optimum

(a)   (b)
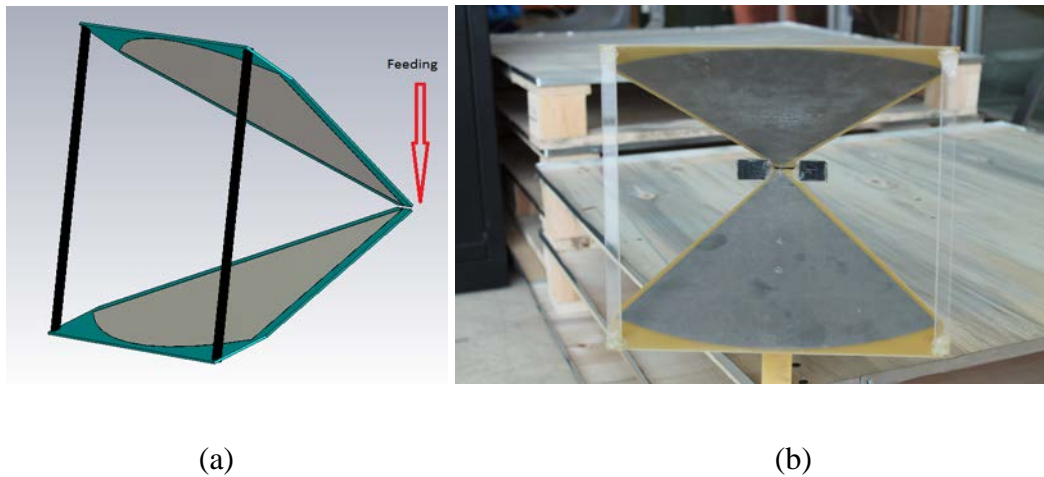
Figure 4.1 The DREBT Antenna a) Simulated antenna b) Realized antenna.

design parameters. Distance between antennas from each other's at the DF array must be considered to obtain the flare angle of the antenna.

Also, mutual coupling of the antennas is one of the other parameter for flare angle (Xiaobo and Zhenghe, 2002). Since higher flare angle decreases the directivity while lower flare angle reduces the band-width, a trade-off is found at 60° for flare angle. The optimum length of each arm is obtained at 25 cm for a port gap of 1mm. To obtain a rigid construction the DREBT antenna is supported with plastic rods between the arms on front side and fixed with plastic supports on the feeding side. The antenna is fed at the port to each arm with a balun circuit which contains an impedance ratio of 1:1.

The realized antenna is measured with the Anritsu MS2037C portable network and spectrum analyzer. Both the measurement and simulation results (CST Microwave Studio and Ansoft HFSS commercial simulation tools) are depicted in Fig. 4.2. As observed in the figure a good agreement is obtained between the simulation and measurement results up to 2.3 GHz while a small discrepancy occurs between 2.3 - 3 GHz regions. The reason for that small discrepancy is probably due to the plastic support rods at the feeding side of the fabricated antennas. A question can arise that the realized S_{11} values are worse for typical commercial DF antennas. But in the application these antennas generally consist of two or more different type of antennas to cover the whole frequency range of interest (e.g. Poynting DF-A0029) whereas we propose a single compact antenna for the whole frequency band. Since the antennas is only used in

receiving mode these return loss values at the frequency band of 150 - 3.000 MHz is satisfactory for a DF application. Despite the fact that a poor impedance matching reduces the captured signals amplitude the noise floor of the receiver is good enough to detect DF application range of interest. The received power level is still acceptable at low frequencies since the path loss between target source and DF system is substantially less at low frequencies than at high frequencies. To improve the impedance matching over the frequency range a matching circuit can be designed by means of capacitors, inductors or PIN diodes (e.g. multi stub tuning) whereas better amplitude values will be shadowed by problems which can arise for the phase of the received signals.
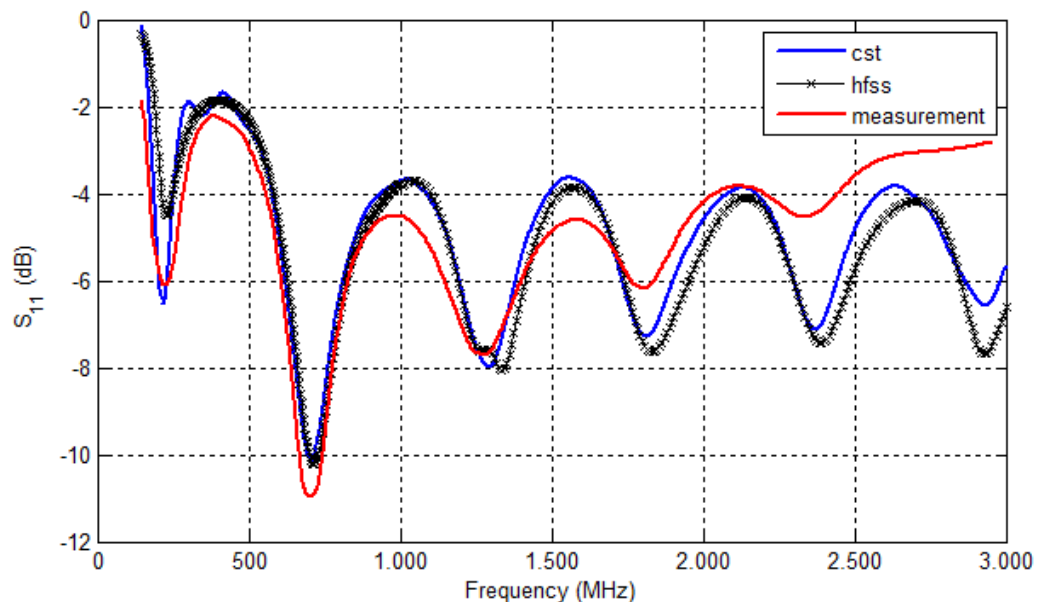
Figure 4.2 The S_{11} Values of The DREBT Antenna.

4.1.2 Direction Finding System Test

We evaluated the performance of the DF system with the proposed DRBET antennas by conducting measurements in an anechoic chamber. In the measurement setup depicted in Fig. 4.3, we performed AoA calculations of the DF system under 5 dB, 10 dB and 15 dB noise. In the anechoic chamber, the turntable was used to turn the DF antenna array between 0° to 359° with 1° incremental steps (Stoddard, 2014). After

that RMS error calculated from the estimated AoA's for all rotated positions. Commercial bi-conical, log-periodic and horn antennas are used as unknown sources. As can be seen in Fig. 4.5, we obtained very good results for the whole frequency band covering from 150 MHz to 3GHz.

It is well known that the number of the antenna elements in the array must be odd and consist of minimum five antennas for accuracy reasons (Jenkins, 1991). To be able to mount on top of a vehicle the whole array radius is restricted to a maximum of 60 cm. The compact size and the performance of the proposed DREBT antenna allowed us to select nine antenna elements to obtain good accuracy of the DF performance taking into account the constraint of 60 cm radius of the circular array.
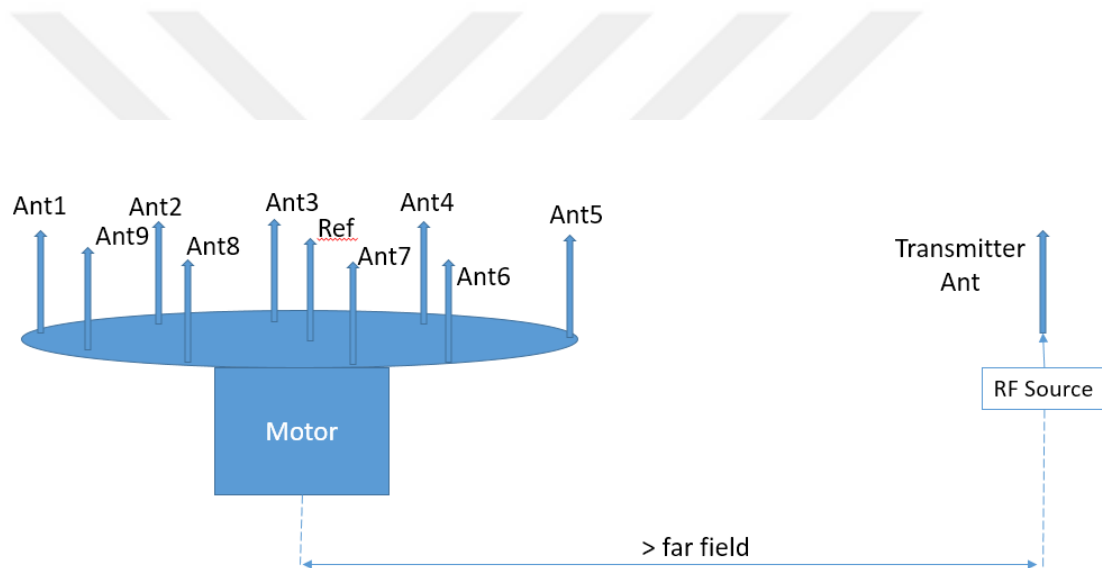
Figure 4.3 DF Test Setup.

Realized wideband DF antenna system is shown in Fig. 4.4. Note that RMS error calculation used is described in chapter 3 under correlative interferometer algorithm section. RMS error is an important tool to compare the direction finding system performances.
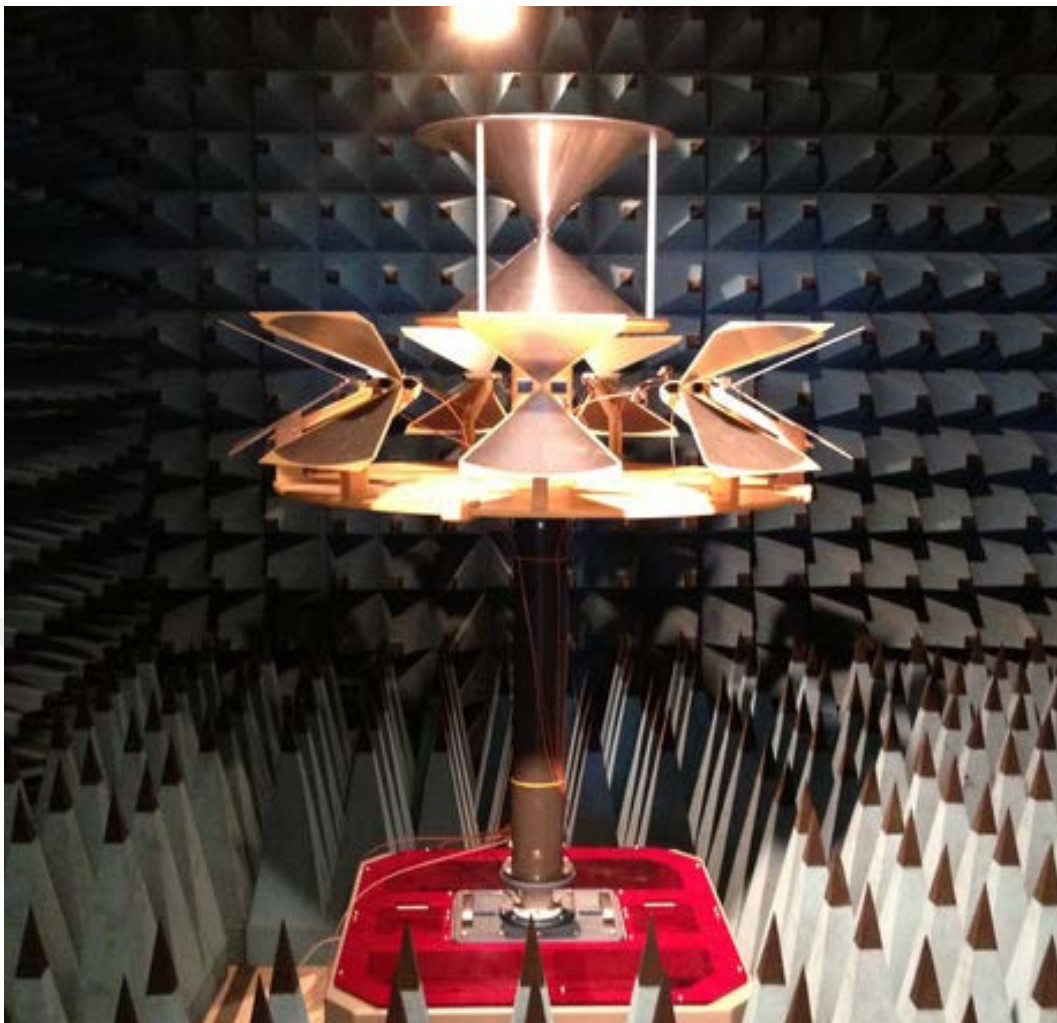
Figure 4.4 DF Antenna System in a Chamber.
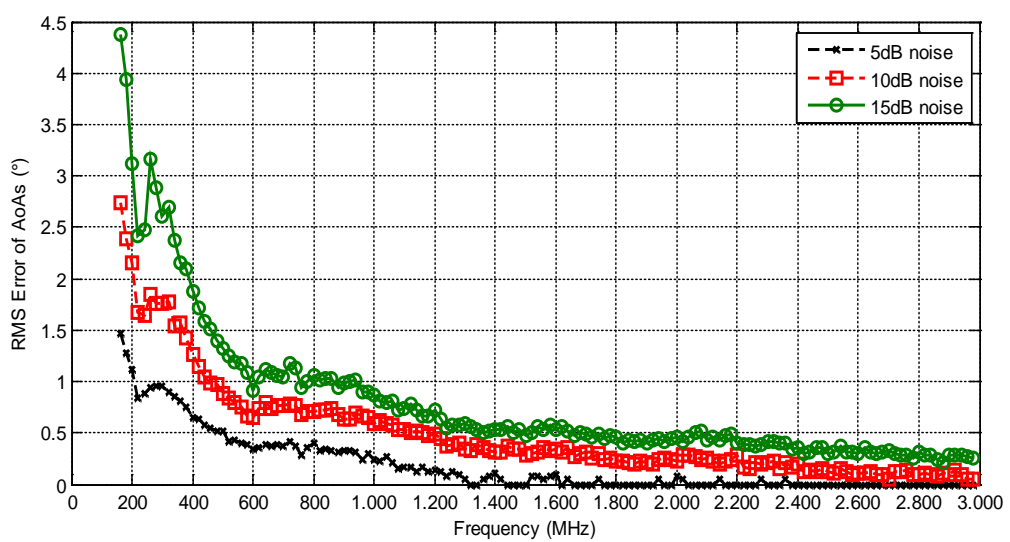
Figure 4.5 RMS DF-Error in a Chamber With Only Interferometer Algorithm.

4.2 OUTDOOR TEST RESULTS

Secondly, we performed outdoor measurements in open field with a mobile DF system mounted on top of a vehicle as shown in Fig. 4.6 (b). The test field is about 4 km^2 forestry rough field with including power lines. In order to have a fair evaluation the system is not only tested for the line of sight but also at different positions including near the power lines, inside the high trees and hills. Diverse test positions were used, e.g., unknown signal source was standing among the high trees or bottom of a hill while DF system was not at line of sight to target the source.

Figure 4.6 DF Antenna System a) DF-A0029 at The Top of The Vehicle b) in a Field at The Top of The Vehicle.

In Fig. 4.7 (a-d), elevation profile of the tests scenarios that are executed from Google Earth program are shown. DF system tests are taken under many test scenarios, some of them are only shown. Distance between two edges, signal source to DF system, is from 244 m up to 1470 m. Altitude is varying from 44 m up to 119 m.

During the tests, 20 samples of AoA's are recorded for all test scenarios. Then, RMS errors of the system are calculated. Measurement are conducted with a 100 MHz frequency step.

a
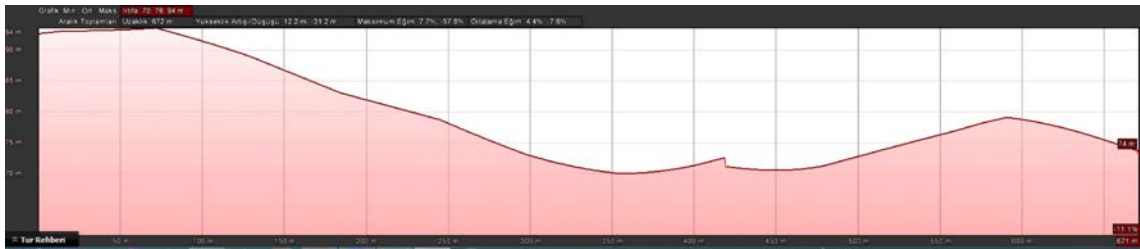
b

c

d

Figure 4.7 DF Test Scenarios (altitude is defined as highest point to lowest point and distance is between source to DF system); a) altitude 62-45 m. and distance 452 m. b) altitude 94-70 m. and distance 671 m c) altitude 78-50 m. and distance 744 m d) altitude 96-47 m. and distance 1.08 km.

As clearly seen in Fig. 4.8, using k-means clustering reduces the DF error. Under 1 GHz, interferometer that only includes phase difference information is performing well. As the frequency increases the distance between the antennas is increasing with respect to the wave length, for frequencies higher than 1 GHz results obtained by only phase difference calculations is not reliable.
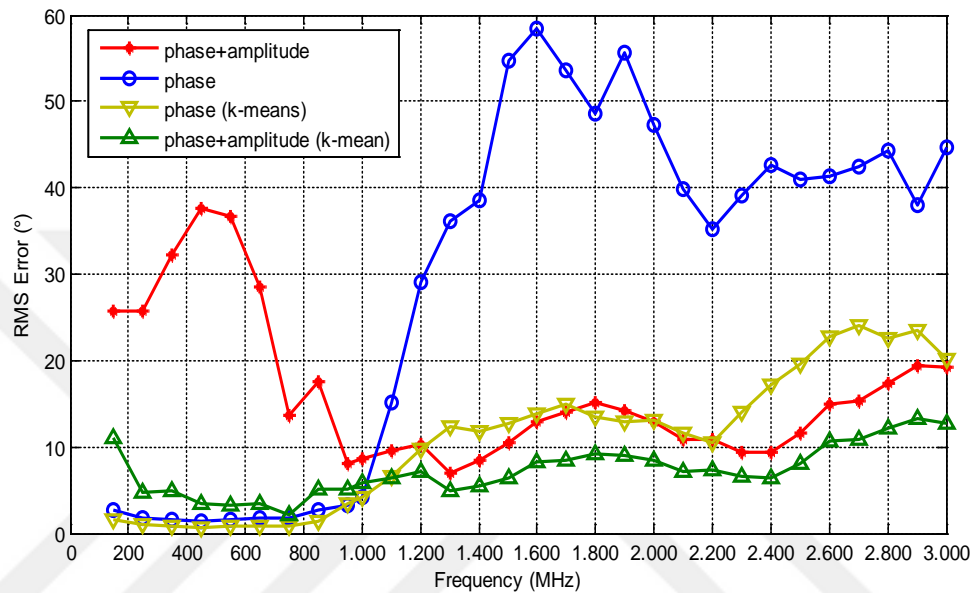
Figure 4.8 RMS DF-Error in Outdoor.

In final step of measurements, a commercial antenna (DF-A0029) that is claimed to work with the interferometer DF algorithm is used from Poynting Inc. The measurements are performed under the same conditions as the proposed DF array antenna. DF-A0029 antenna covers all the tested frequencies with two different array antennas that contain dipole antennas for 150 MHz to 1 GHz and monopole antennas for 1 GHz to 3 GHz. Test results of DF-A0029 antenna and comparison with proposed antenna are shown in Fig. 4.9. As can be seen in Fig. 4.9 the proposed antenna in general performs better than the measured commercial antenna for a DF application.
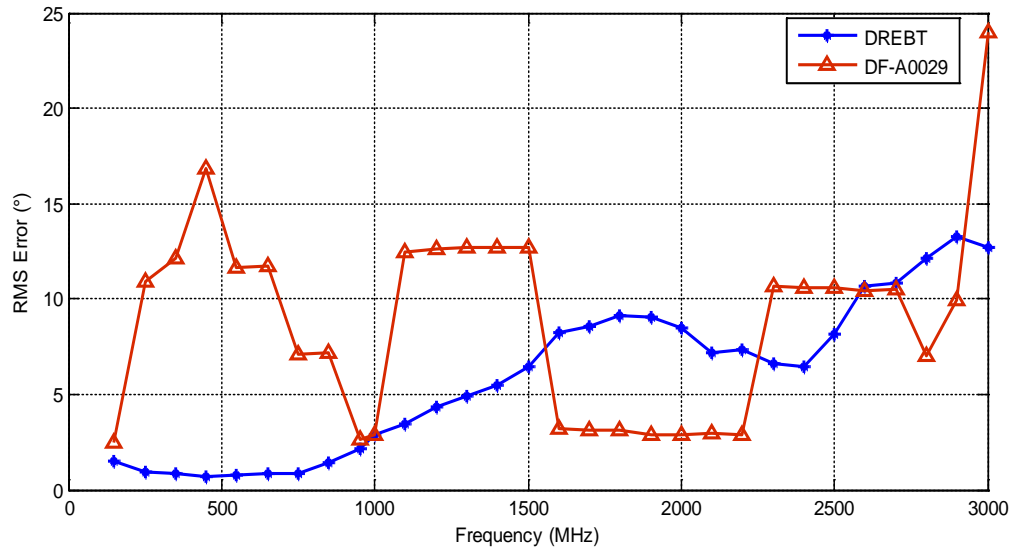
Figure 4.9 RMS DF-Error of Poynting DF-A0029 vs DREBT.

CHAPTER 5

IMPLAMENTATION OF A MUSIC ALGORITHM

5.1 SIGNAL AND NOISE MODEL

Emitted signals from the transmitter distributions are assumed to be identical. Signs zero mean, regardless of the noise, is uncorrelated. Signal and noise will be represented by complex Gaussian probability distribution (Astely and Ottersten, 1999).

Signal needs to be narrow band that requires adequate sampling rate since during the transfer the digital environment should not be any loss of information. Therefore, original source signals can be retrievable from emitted signals (Barabell, 1983).

Multiple reflections from the ambient needs to be neglected, the positioning error arising from this effect has to be taken into account. All signs in different ways to reach out to the receiver system undergoes multiple reflections from a transmitter has to deemed fully or partially correlation with each other (Corbin 2011).

Noise can be divided into two classes, emanating from the receiver and the external environment. Receiver internal noise is zero mean Gaussian and is considered uncorrelated with each other. Ideal conditions in the power of noise generated in each receiver will be equal, but unequal situations may also occur. Receivers' noises are assumed to be both temporal and spatial static noise with white noise. Also, Gaussian of zero average ambient noise is assumed to be both temporal and spatial static noise with white noise (Dadgarpour et al., 2015).

5.2 USED ARRAY ANTENNA AND ENVIRONMENT MODEL

Antennas are regarded as spatial filters, on the one hand enhancing the signal from the desired direction while on the other hand suppressing the signals from the other directions. SNR in passive antenna combination is proportional to the number of antennas in general. Affecting the performance of the antenna combination from the same antenna elements are composed of two main factors. These are the geometry of the antenna array (linear, circular, etc.) and the distance from the antenna to each other (Hertl and Strycek, 2007).

In the DF antenna system, number of the antenna is intended for use as small as possible. As the number of antennas increasing the processing overhead and system costs increases. Nevertheless, the operating performance of the DF system is also increasing. This is why the relationship between the numbers of antenna systems with performance requirements should be balanced (Hui, 2003).

DF systems, that use MUSIC algorithm in ships, generally has the horizontally linear array antennas with a coverage of a maximum 180 degrees horizontal angle range. However, this system is operated with 120 degrees horizontal angle range to prevent DF system from front-rear direction confusion. If vertical angle of AoA is needed, second linear antenna array is placed vertically. Both horizontally and vertically linear antenna array of DF systems are operated independently from each other (Kim and Viberg, 1996).

Proposed array antenna of each element will be identical and vertically polarized, it has to insensitive for horizontally polarized signals. Determination of the correct orientation of the antenna matrix combinational methods which will be used in the implementation is very important. Routing matrix of uniform linear antenna lineup is as follows:

$$
A(\theta) = \begin{bmatrix} 1 & \cdots & 1 \\ e^{2\pi d Sin(\theta_1)} & \cdots & e^{2\pi d Sin(\theta_D)} \\ \vdots & \cdots & \vdots \\ e^{2\pi(M-1)Sin(\theta_1)} & \cdots & e^{2\pi(M-1)Sin(\theta_D)} \end{bmatrix} \tag{5.1}
$$

where θ_D is AoA of source that is numbered D and $-\pi/2 < \theta_D < \pi/2$.

As seen at Fig. 5.1, M number of antenna linearly lineup with index of $i = 1,2,3…M$ at x axis. A single frequency signal, $s(i,t)$, is assumed as,

$$s(i,t) = V \cos(2\pi f (t - \tau_i))$$
(5.2)

where f is frequency, V is amplitude of the signal and τ_i is time delay with respect to i that is defined as

$$\tau_i = id \sin(\theta) / c$$
(5.3)

where d is distance between antennas and c is light speed at free space.
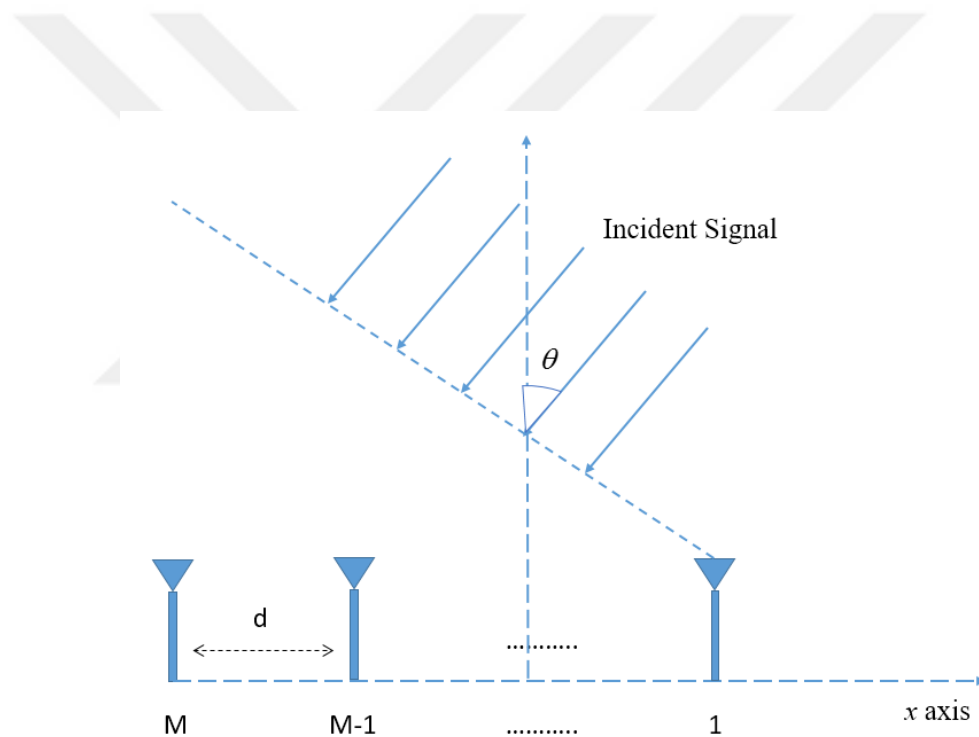
Figure 5.1 Representation of Plane Waves with Linear Antenna Arrays.

From combination of both equation 5.2 and 5.3, result will be

$$s(i,t) = V \cos(2\pi f (t - id \sin(\theta) / c))$$
(5.4)

Number of K emitted signals from the source to follow different paths undergoes multiple reflections and number of D will reach a different way to receiver system. M number sequence obtained by the antenna element signals, D are a sign of narrow-band linear composition. This information can be obtained using the modeling sign $\mathbf{y}$ antenna output signal as a first step.

$$\mathbf{y} = \mathbf{A}\mathbf{s} + \mathbf{g} \tag{5.5}$$

$$\begin{bmatrix} y_1 \\ y_2 \\ \vdots \\ y_M \end{bmatrix} = \begin{bmatrix} a_1(\theta_1) & a_1(\theta_2) & \cdots & a_1(\theta_D) \\ a_2(\theta_1) & a_2(\theta_2) & \cdots & a_2(\theta_D) \\ \vdots & \vdots & \cdots & \vdots \\ a_M(\theta_1) & a_M(\theta_2) & \cdots & a_M(\theta_D) \end{bmatrix} \begin{bmatrix} s_1 \\ s_2 \\ \vdots \\ s_M \end{bmatrix} + \begin{bmatrix} g_1 \\ g_2 \\ \vdots \\ g_M \end{bmatrix} \tag{5.6}$$

where $\mathbf{y}$ is the antenna output signal, $\mathbf{A}$ is mode matrix, $\mathbf{s}$ is incident signal vector that includes amplitude and phase information relative to a reference point set in sequence from the antenna signals and $\mathbf{g}$ is the noise vector.

Multiplication of $\mathbf{A}$ and $\mathbf{s}$ will comprise the total signal resulting effect of each antenna. And, with addition of $\mathbf{g}$ the antenna output signal is defined. From Fig. 5.1, $a_m(\theta_d)$ depends on position of antenna in the array and angle of arrival signal. Now we define $a_m(\theta_d)$ as

$$a_m(\theta_d) = e^{-i2\pi(m-1)d\sin(\theta_d)/\lambda} \tag{5.7}$$

Column vectors of matrix $\mathbf{A}$ is named wavefront vector that contains the signal information. So the total desired signal will be

$$\mathbf{x} = \mathbf{A}\mathbf{s} = \sum_{l=1}^{D} \mathbf{a}(\theta_l)\mathbf{s}_l \tag{5.8}$$

Therefore in the antenna output the observed signal (Eq. 5.5) becomes

$$\mathbf{y} = \mathbf{x} + \mathbf{g} \tag{5.9}$$

Antenna array data can be written as

$$\mathbf{R}_{yy} = E\left[\mathbf{y}\mathbf{y}^H\right] \tag{5.10}$$

where $E[.]$ is the expected value and '$\mathbf{y}^H$' is the Hermit equivalent of $\mathbf{y}$. Practically, this matrix is written with N number of array antenna $y_n \{n = 1, 2, \ldots, N\}$

$$\mathbf{R}_{yy} = \frac{1}{N}\sum_{n=1}^{N}\mathbf{y}_n\mathbf{y}_n^H \tag{5.11}$$

Then, signal-noise model is applied as,

$$\mathbf{R}_{yy} = \mathbf{A}\mathbf{P}\mathbf{A}^H + \sigma_n^2\mathbf{I} \tag{5.12}$$

where $\mathbf{P} = E\left[\mathbf{s}\mathbf{s}^H\right]$ if Eq. 5.8 is considered and $\mathbf{R}_{xx} = E\left[\mathbf{x}\mathbf{x}^H\right] = \mathbf{A}\mathbf{P}\mathbf{A}^H$. Also, white noise spatial assumptions is $\mathbf{R}_{gg} = E\left[\mathbf{g}\mathbf{g}^H\right] = \sigma_n^2\mathbf{I}$. If $\mathbf{P}$ is not single, $\mathbf{R}_{yy}$ must be positive and Hermit structure;

$$\mathbf{P} = E\left[\mathbf{s}\mathbf{s}^H\right] = Diag\left[P_1, P_2, \ldots, P_D\right] \tag{5.13}$$

$P_k = s_k^2$ is signal power that is from the direction of θ_k. $\mathbf{R}_{xx}$ can be obtained from Eq. 5.6, $\mathbf{a}_k = \left[a_1(\theta_1), a_2(\theta_2), \ldots, a_M(\theta_k)\right]^T$ with P_k

$$\mathbf{R}_{xx} = \sum_{k=1}^{D} P_k\mathbf{a}_k\mathbf{a}_k^H \tag{5.14}$$

Also, $\mathbf{R}_{xx}$ can be defined with eigenvalues λ_k and eigenvalue vectors $\mathbf{v}_k$;

$$\mathbf{R}_{xx} = \sum_{k=1}^{M} \lambda_k\mathbf{v}_k\mathbf{v}_k^H = \sum_{k=1}^{D} \lambda_k\mathbf{v}_k\mathbf{v}_k^H \tag{5.15}$$

Besides, M dimensional matrix can be expressed with D dimensional. In this case, eigenvalues of $\lambda_{D+1}, \ldots, \lambda_M$ is equal to zeros. Also, noise can be defined with eigenvalues that is written as Eq. 5.16 and total relationship is written in Eq. 5.17 as,

$$\mathbf{R}_{gg} = \sigma_n^2 \mathbf{I} = \sigma_n^2 \sum_{k=1}^{M} \mathbf{v}_k \mathbf{v}_k^H \tag{5.16}$$

$$\mathbf{R}_{yy} = \sum_{k=1}^{D} \lambda_k \mathbf{v}_k \mathbf{v}_k^H + \sigma_n^2 \sum_{k=1}^{M} \mathbf{v}_k \mathbf{v}_k^H$$
$$= \sum_{k=1}^{D} \left(\lambda_k + \sigma_n^2 \right) \mathbf{v}_k \mathbf{v}_k^H + \sigma_n^2 \sum_{k=D+1}^{M} \mathbf{v}_k \mathbf{v}_k^H \tag{5.17}$$

Eigenvalues are illustrated in Fig. 5.2.
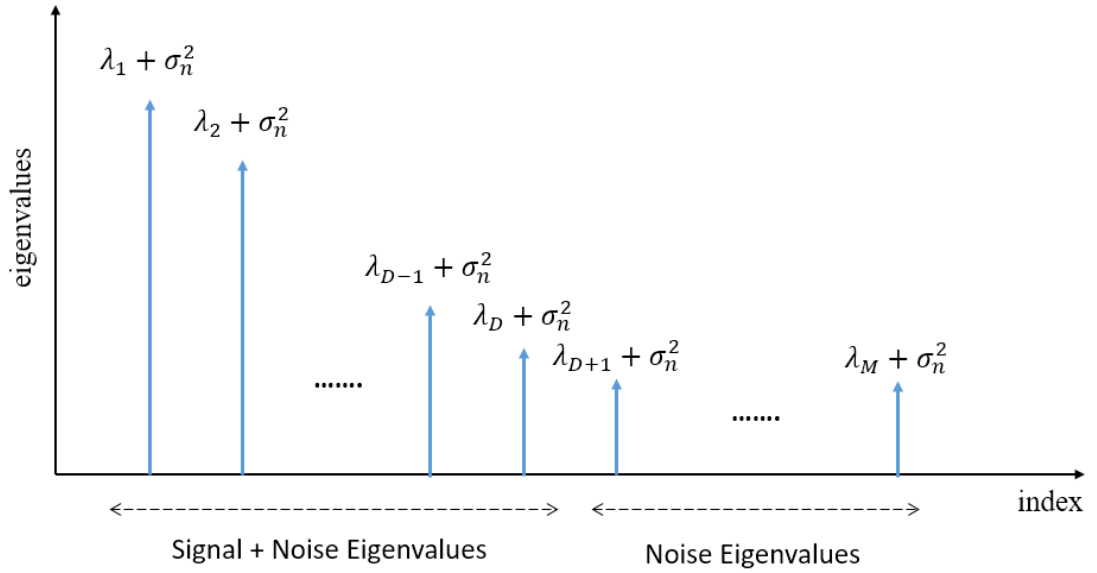
Figure 5.2 Representation Signal and Noise Eigenvalues.

Eigenvalues of $\mathbf{R}_{yy}$ split into two disjoint cluster as seen in Fig. 5.2. When the signal and noise eigenvalues are perpendicular, subspace of signal and noise vectors are also perpendicular to each other. Therefore, $\mathbf{a}(\theta_k)$, mode vector is perpendicular to all eigenvalues.

$$\mathbf{a}^H \left(\theta_1 \right) \mathbf{v}_i = 0, \quad k = 1, 2, \ldots, D \quad i = D+1, \ldots, M \tag{5.18}$$

Eq. 5.18 is used to get MUSIC spectrum. In this way, angle of incidence, θ, can be determined.

$$\sum_{k=D+1}^{M} \mathbf{a}^{H}(\theta) \mathbf{v}_{k} = 0 \tag{5.19}$$

Eq. 5.19 gives the solution of θ with number of D. Power relationship with respect to angle is given by,

$$P_{xx}(\theta) = \sum_{k=D+1}^{M} \left| \mathbf{a}^{H}(\theta) \mathbf{v}_{k} \right|^{2} \tag{5.20}$$

Finally, the MUSIC spectrum (Saraç et al., 2008b) can be defined as

$$
\begin{aligned}
P_{xx}^{MUSIC}(\theta) &= \frac{1}{P_{xx}(\theta)} \\
&= \frac{1}{\sum_{k=D+1}^{M} \left| \mathbf{a}^{H}(\theta) \mathbf{v}_{k} \right|^{2}} \\
&= \frac{1}{\mathbf{a}^{H}(\theta) \mathbf{v}\mathbf{v}^{H} \mathbf{a}(\theta)}
\end{aligned}
\tag{5.21}
$$

5.3 EXAMPLES OF MUSIC IMPLEMENTATION

MUSIC algorithm is implemented with eight monopole antenna that is linearly sequences as seen in Fig. 5.1. During the implementation, eight receiver is used. MUSIC spectrum is seen in Fig. 5.3 that has result of one unknown source signal application. Unknown signal position with respect to is at the 127° azimuth and 75° elevation.

Fig. 5.4 has two different but at the same frequency that is 100 MHz unknown signal in test environment. Unknown signal sources are; 213° azimuth, 105° elevation and 57° azimuth, 80° elevation. Fig. 5.5 has two different but at the same frequency that is 500 MHz unknown signal in test environment. Unknown signal sources are; 213° azimuth, 105° elevation and 57° azimuth, 80° elevation. Fig. 5.6 has two different but at
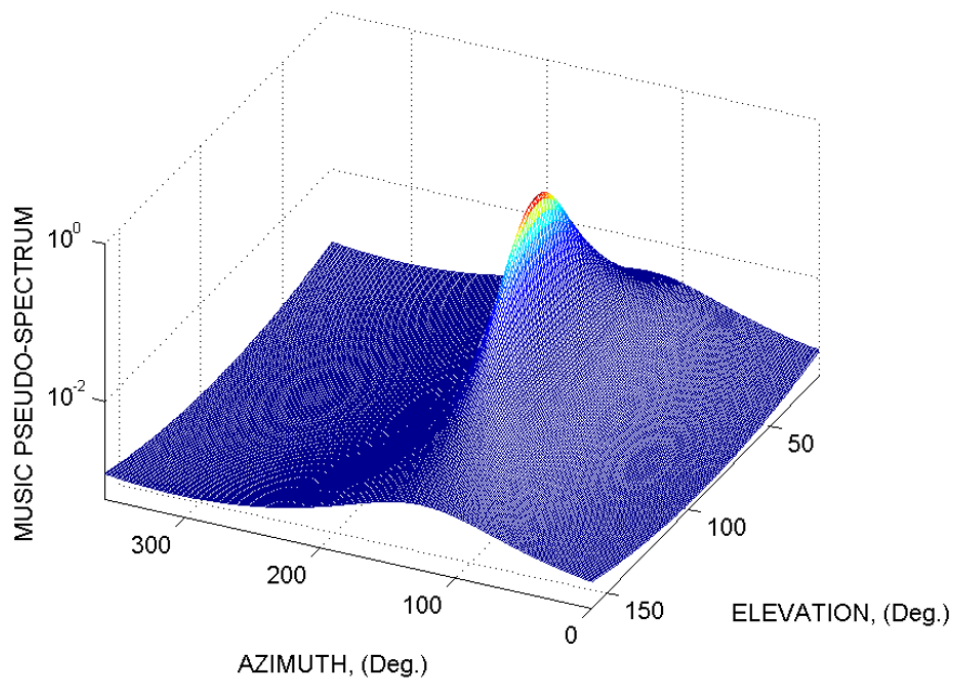
Figure 5.3 MUSIC Spectrum for f =100 MHz with Single Unknown Signal Source.
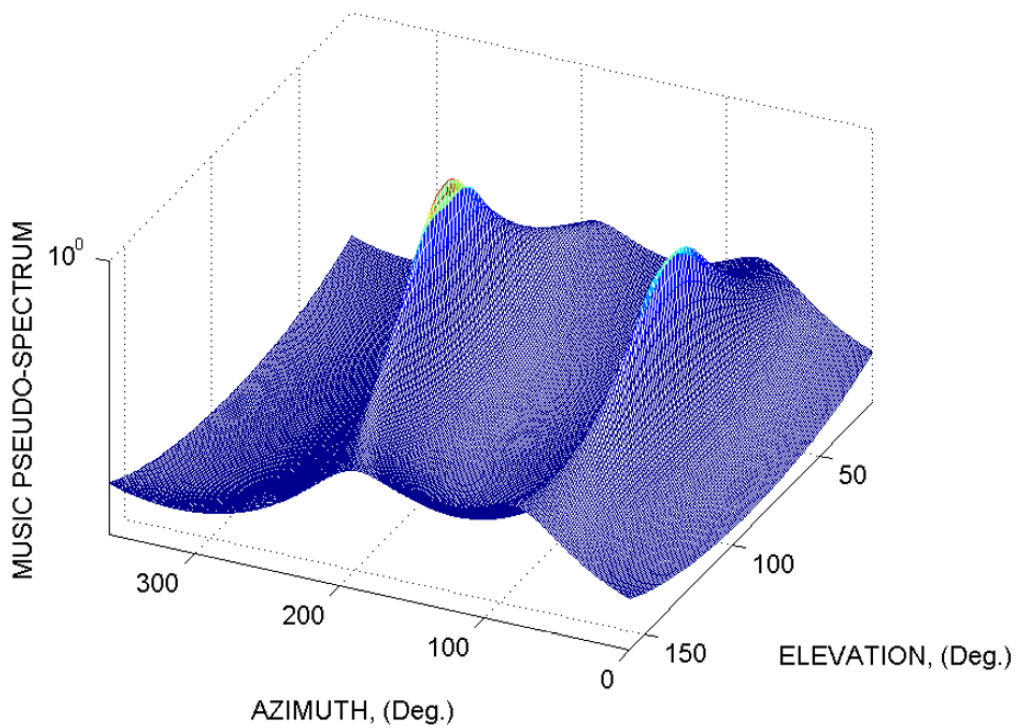
Figure 5.4 MUSIC Spectrum for f =100 MHz with Two Different Unknown Signal Source.
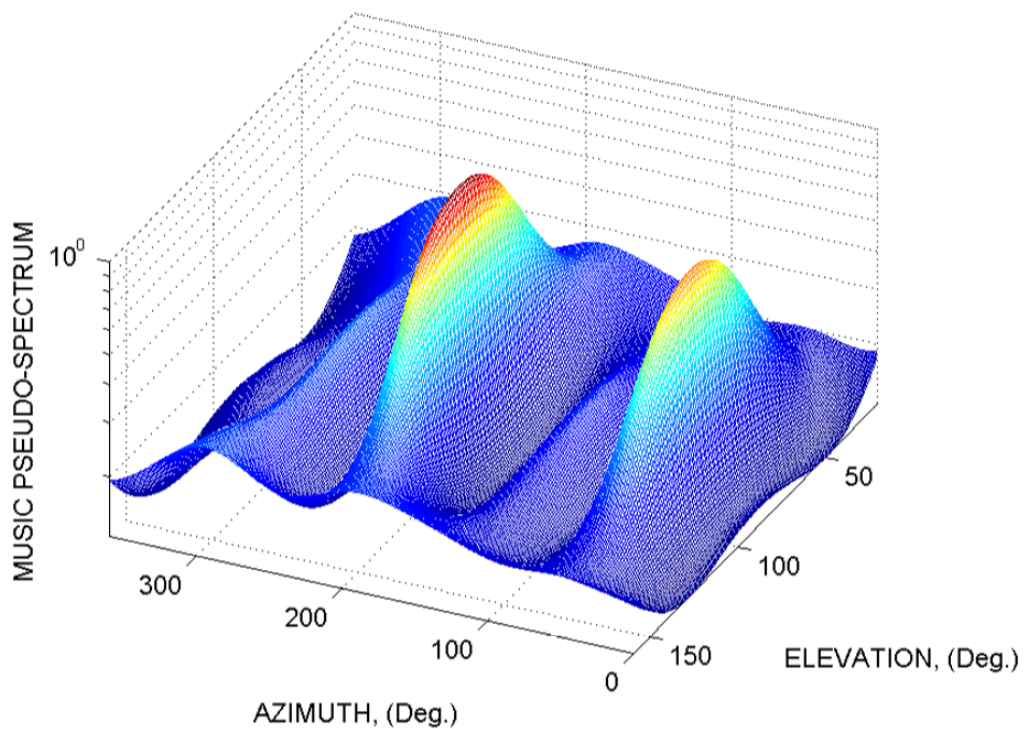
Figure 5.5 MUSIC Spectrum for f =500 MHz with Two Different Unknown Signal Source.
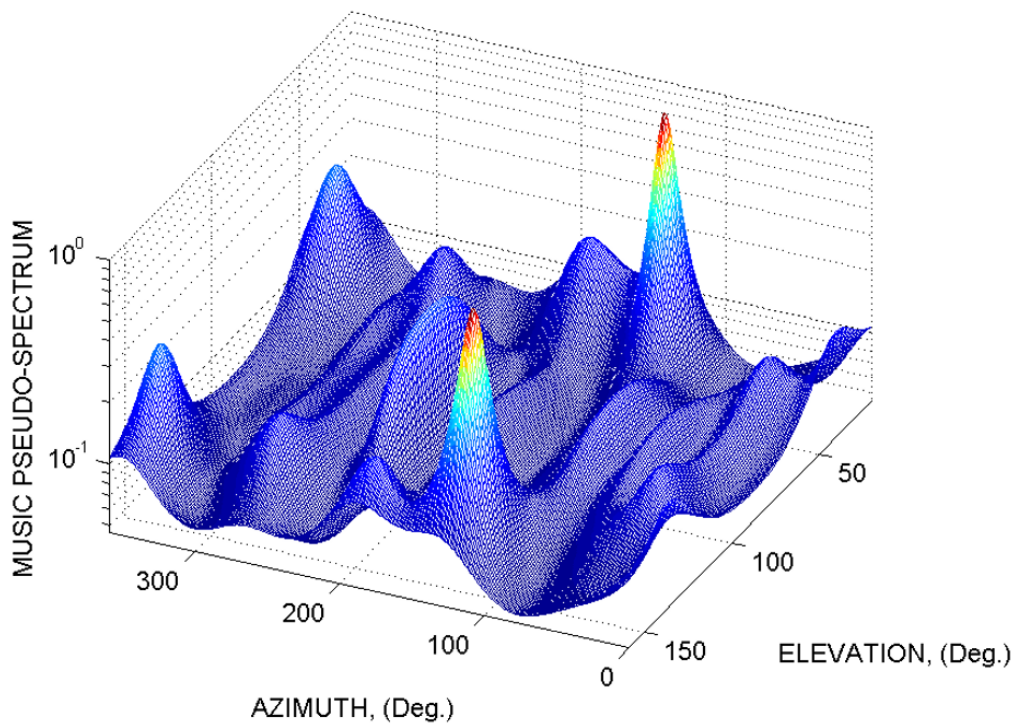
Figure 5.6 MUSIC Spectrum for f =900 MHz with Two Different Unknown Signal Source

the same frequency 900 MHz unknown signal in test environment. Unknown signal sources are; 213° azimuth, 105° elevation and 57° azimuth, 80° elevation.

As seen from examples, with using MUSIC algorithm, two different unknown signal could be detected while other algorithms not. Despite that, MUSIC algorithm cannot be used for wideband applications (Wu et al., 1995).

We have to mention that we could not apply the MUSIC algorithm for the measurement setup explained in chapter 4. The reason for that, proposed setup has two receivers which means, signals at the all antenna elements of array cannot be read from receivers at the same time. To achieve that, number of receivers should be equal to number of antennas at the array. In addition that, MUSIC algorithm is not enough to calculate AoA while structure of antenna array is different from linear.

CHAPTER 6

CONCLUSIONS

DF systems have widely usage area. It has very important place in technology. DF systems are used by military, civilian and research centers. Air and marine navigation, search and rescue, personnel and vehicle locators, frequency management and wildlife tracing are some of DF system usage areas. Different DF algorithms are developed up to todays. As described in chapter two, amplitude based, phase based and super resolution methods are made progress.

In this thesis, the development of a novel single antenna element and set up of a mobile DF application is aimed. A compact DREBT antenna as a single element of a DF array antenna is designed and manufactured that is operating from 150 MHz to 3 GHz for mobile DF systems. The performance of the proposed antenna is evaluated in a DF system both in an ideal measurement setup in an anechoic chamber and in open fields. The measurements in open field were conducted not only at the line of sights but also at different conditions to obtain a fair evaluation. The results in chapter 4 show the novelty of the proposed antenna. In addition the developed whole DF system is also used by a commonly used commercial DF antenna to compare and validate the superiority and novelty of the proposed antenna in open field.

The measurement results verify that the proposed DREBT antenna is a novel single antenna element for mobile DF applications especially when considering its size, weight and easy manufacturing. Besides, proposed antenna has directional radiation pattern that makes possible to use not only the phase comparison estimation methods to calculate AoA. Amplitude based estimation techniques can also be operated on the

proposed DF array antenna which is also implemented and the results are reported.

Because of the narrow radiation characteristics of the proposed DREBT at high frequencies, when combining the amplitude estimation techniques with phase estimation techniques give the better result at high frequencies. On the other hand, the results show that the single phase estimation technique is more suitable for lower frequencies.

In this thesis, not only the antenna is developed but also the whole mobile DF system is proposed. As described in chapter three, all hardware and software parts of the mobile DF system is established. During the studies, omni-directional loaded bi-conical antenna that operates at interested frequency range is designed. Correlative interferometer that depends on phase of the signal is used with k-means clustering algorithm. Also, triangulation algorithms, that are discussed in chapter three, is used with open source map user interface to locate the unknown signal source.

Additionally, MUSIC algorithm that is described in the chapter five, is discussed. MUSIC algorithm has some advantages over other DF methods if there are more than one unknown signal source which have a radiation at the same frequency. However, MUSIC algorithm is applied to different antennas and array sequence that makes the situation impossible to compare with proposed DREBT antenna array and used algorithm.

Further studies will cover different frequency range with different DF algorithms. New antenna could be designed with respect to different interested frequency range. Also, different antenna sequences could be tried with MUSIC algorithm.

REFERENCES

Astely, D. and Ottersten, B., "The Effect of Local Scattering on Direction of Arrival Estimation with MUSIC", *IEEE Transaction on Signal Proccesing.*, Vol. 47, no.12, pp. 3220-3234, 1999.

Bailey, M.C., Campbell, T.G., Reddy, C.J., et al., "Compact Wideband Direction-Finding Antenna", *Antennas and Propagation Magazine, IEEE,* vol.54, no.6, pp.44-68, December 2012.

Balanis, C.A., *Antenna Theory Analysis and Design,* John Wiley & Sons Press, 3rd edn, 2005.

Barabell, A. J., "Improving The Resolution Performance of Eigen Structure Based Direction-Finding Algorithm", *IEEE ICASSP*, Boston, pp. 345353, 1983.

Cho, C., Park, I., Choo, H., "Design of a Small Antenna for Wideband Mobile Direction Finding Systems", *IET Microw. Antennas Propag.*, Vol. 4, Iss. 7, pp. 930-937, 2010.

Corbin, C.F., *High Frequency Direction Finding Using Structurally Integrated Antennas On A Large Airborne Platform*, M.S. Thesis, Air University, 2011.

Dadgarpour, A., Zarghooni, B., Virdee, B., et al., "Millimeter-Wave High-Gain SIW End-Fire Bow-tie Antenna", *IEEE Transaction on Antenna And Propagation*, vol.63, no.5, 2015.

Ghosh, D., Sarkar, T. K., Mokole, E. L., "Design of A Wide-Angle Biconical Antenna for Wideband Communications", *Progress In Electromagnetics Research B*, Vol. 16, 229-245, 2009.

Friedlander, B. and Ksienski, A. J., "Direction Finding In The Presence of Mutual Coupling", *IEEE Transactions on Antennas and Propagation*, Vol. 39, no. 3, pp. 273-284, 1991.

Hertl, I., Strycek, M., "UWB Antennas for Ground Penetrating Radar Application", *Applied Electromagnetics and Communications, 19th International Conference*, pp.1-4, 24-26 Sept. 2007.

Hui, H.T., "Improvement Compensation for the Mutual Coupling Effect in a Dipole Array for Direction Finding", *IEEE Trans. On Antennas and Propag.*, Vol. 51, No.9, 2003.

Jahoda, J.R., "Miniature Direction-Finding Antenna Array", *LLC, High Frequency Electronics*, 2007.

Jenkins, H. H., *Small-Aperture Radio Direction-Finding*, Artech House Inc., 1991.

Johnson, D.H., "The Application of Spectral Estimation Methods to Bearing Estimation Problems", *Proceedings of the IEEE*, vol.70, no.9, pp.1018-1028, Sept. 1982.

Karacolak, T., Topsakal, E., "A Double-Sided Rounded Bow-Tie Antenna for UWB Communication", *IEEE Antennas and Wireless Propagation Letters*, vol.5, 2006.

Kebeli, M., "Extended Symmetrical Aperture Direction Finding Using Correlative Interferometer Method", *Electrical and Electronics Engineering (ELECO), 2011 7th International Conference on*, pp.II-209-213, 1-4 Dec. 2011.

Kellogg, R.L., Mack, E.E, Crews, C.D., "Direction Finding Antennas and Systems", in Volakis, J.L. (Ed.): *Antenna Engineering Handbook*, McGraw-Hill Press, 4th edn., pp. 1403-1435, 2007.

Kennedy, J., Sullivan, M.C., "Direction Finding and Smart Antennas Using Software Radio Architectures", *Communications Magazine, IEEE*, vol.33, no.5, pp.62-68, May 1995.

Krim, H., Viberg M., "Two Decades of Array Signal Processing Research: The Parametric Approach", *Signal Processing Magazine, IEEE*, vol.13, no.4, pp.67-94, Jul 1996.

Ku-Ting, L., *Comparison of Superresolution Algorithms with Different Array Geometries For Radio Direction Finding*, M.S. Thesis, Naval Postgraduate School, 1998.

Le-ngoc, S., Le-ngoc, T., "Precision Direction Finding Antennas", *IEEE Trans. Consum. Electron.*, 36, pp. 918-921, 1990.

Liang, X., Chia, Y.W.M., "New Precision Wideband Direction Finding Antenna", *IEEE Proc. Microw. Antennas Propag.*, 148, pp. 363-364, 2001.

Liberal, I., Cartelli, D., Yarovoy, A., "Conformal Antenna Array for Ultra-Wideband Direction-of-arrival Estimation", *Int. Journal of Microw. and Wireless Tech.*, pp 1-12, 2011.

Lim, E.G., Wang, Z., Lei, CU., et al., "Ultra Wideband Antennas – Past and Present", *IAENG International Journal of Computer Science*, v. 37 n. 3, p. 304-314, 2010.

Stoddard, R.E., *Direction Finding Using Antenna Array Rotation*, US Patent No. US2014/0159954 A1, 2014.

Mueller, R., at al., "A UHF Ultra Broadband Vivaldi-Type Direction Finding Antenna", *Antennas and Propagation Society International Symposium (APSURSI), IEEE,* pp.1-4, 11-17 July 2010.

Mueller, R., Fuchs, C., Lorch, R., et al., "A Conformal UHF Slot Type Direction Finding Antenna with Optimized Radar Cross Section", *Antennas and Propagation Society International Symposium, 2009. APSURSI '09. IEEE,* vol., no., pp.1-4, 1-5 June 2009.

Mueller, R., Lorch, R., Menzel, W., "A UHF Direction Finding Antenna with Optimised Radar Cross Section", *Antennas and Propagation Society International Symposium 2006, IEEE*, vol., no., pp.3255-3258, 9-14 July 2006.

Ozer, H., Yapanel, U., Olcer, I. et al., "Classification of Transient Signals Using Hierarchical Wavelet Decomposition", *RCMCIS'2000*, Zegrze, Poland, 2000.

Ozturk, M.E., Kebeli, M., "Comparison of The Directed Bow-Tie Antenna Types For Direction Finding at UHF", *Antennas and Propagation Society International Symposium (APSURSI), 2013 IEEE*, pp.1302, 1303, 7-13 July 2013.

Ozturk, M.E., Kebeli, M., "Directed Rounded-Edge Bow-Tie Antenna for Direction Finding at Ultra High Frequencies", *Radio Science Meeting (Joint with AP-S Symposium), 2013 USNC-URSI*, pp.98, 7-13 July 2013.

Ozturk, M.E., Korkmaz, E., Kebeli, M., "Rounded-Edge Bow-Tie Antenna for Wideband Mobile Direction Finding System", *IET Microwaves, Antennas & Propagation*, Vol. 2015/9, No. 15, pp. 1751-8733, Dec. 2015.

Park, C.S., Kim, D.Y., "The Fast Correlative Interferometer Direction Finder using I/Q Demodulator", *IEEE Asia-Pacific Conference on Communications, APCC'06*, pp.1-5, Aug. 2006.

Pascal, C., "A Direction Finding Method Under Sensor Gain And Phase Uncertainties", *IEEE Transaction on Signal Processing*, Vol. 44, no. 5, pp.3045-3054, 2000.

Paulraj, A. and Kailath, T., "Direction of Arrival Estimation by Eigen Structure Methods with Unknown Sensor Gain And Phase", *IEEE ICASSP*. Tampa, FL, pp. 640-643. 1985.

Pierre, J. and Kaveh, M., "Experimental Performance Of Calibration And Direction-Finding Algorithms", *IEEE ICASSP.*, Toronto, Canada. Vol. 2, pp.1365-1368, May, 1991.

Poor, H. V., *An Introduction To Signal Detection And Estimation*. Springer, New York, 1994.

Sandler, S.S., King, R.W.P., "Compact Conical Antennas for Wide-Band Coverage", *IEEE Trans. On Antennas and Propag.*, Vol. 42, No.3, 1994.

Saraç, U., *Detection and Localization of Multiple Emitters in The Presence of Multipath*, Ph.D. Thesis, ITU, 2009.

Saraç, U., Harmancı, F. K. ve Akgül, T., "Detection And Localization of Emitters In The Presence of Multipath Using A Uniform Linear Array", *The Fifth IEEE Sensor Array and Multichannel Signal Processing Workshop (SAM)*, pp. 419-422, Darmstadt, Germany, 21-23 July, 2008.

Saraç, U., Harmancı, F. K. ve Akgül, T., "Experimental Analysis of Detection And Localization of Multiple Emitters In Multipath Environments", *IEEE Antennas and Propagation Magazine*, Vol. 50, No. 5, pp. 61-70, 2008.

Schmidt, R. O., "Multiple Emitter Location And Signal Parameter Estimation", *IEEE Transactions on Antennas and Propagation*, Vol. AP-34, no. 3, pp. 276-280, 1986.

Shan, T., Wax, M., and Kailath, T., "On Spatial Smoothing of Direction of Arrival Estimation of Coherent Signals", *IEEE Transactions on Acoustics, Speech, and Signal Processing*, Vol. ASSP-33, no. 4, pp. 806-811, 1985.

Tan, K. and Zhang, M., "Signal Enumeration And Direction-Of-Arrival Estimation For Coherent Signals In Correlated Noise With Unknown Parameters", *Proceedings of ICSP.*, pp. 339-342, 1998.

Thomas, S. and Matties, W., "High-Resolution Direction Finding Using A Switched Parasitic Antenna", *IEEE Transaction on Signal Processing*, Vol. 45, no.11, pp. 1223-1232, 2001.

Vaseghi, S. V., *Advanced Signal Processing And Digital Noise Reduction*, Wiley&Teubner, New York, 1996.

Wax, M. and Sheinvald, J., "Direction Finding of Coherent Signals Via Spatial Smoothing For Uniform Circular Arrays", *IEEE Transaction on Antennas and Propagation*, Vol. 42, no. 5, pp. 613-620. 1994.

Wu, Y. W., "Estimation Directions of Arrival With Generalized MUSIC Using A Linear -Interpolated Array Manifold", *IEEE ICASSP*, Vol. 5, pp. 3333-3336, 1991.

Wu, Y. W., Rhodes, S. and Satorius, E. H., "Direction of Arrival Estimation via Extended Phase Interferometry", *IEEE Transaction on Aerospace and Electronics Systems*, Vol. 31, no. 1, 1995.

Xiaobo, A., Zhenghe, F., A Single Channel Correlative Interferometer Direction Finder Using VXI Receiver", *3rd International Conference on Microwave and Millimeter Wave Technology Proceedings, ICMMT 2002*, pp.1158-1161, 17-19 Aug. 2002.

Yeo, J., Lee, J., "Miniaturized LPDA Antenna for Portable Direction Finding Applications", *ETRI Journal*, Vol. 34, No. 1, February 2012.

Yong, G., Ci, X. X. and Zhong, Z. Z., "Erasing False-Location of Two Stations Direction-Finding Cross Location in Multi-Path And Multiple Sources Environments", *CIE International Conference on Proceedings*, pp. 864-868, 2001.

Zhou, R., Zhang, H., Xin, H., "Improved Two-Antenna Direction Finding Inspired by Human Ears", *IEEE Trans. On Antennas and Propag.*, Vol. 59, No.7, 2011.

Zhou, Y., "Emitter Number Detection Based On Clustering And The Application of Information Theoretic Criteria". *IEEE Transactions on Acoustics, Speech, and Signal Processing*, Vol. SAM.4.12, pp. 1021-1024, 2005.

APPENDIX A

DECLARATION STATEMENT FOR THE ORIGINALITY OF THE THESIS, FURTHER STUDIES AND PUBLICATIONS FROM THESIS WORK

A.1 DECLARATION STATEMENT FOR THE ORIGINALITY OF THE THESIS

I hereby declare that this thesis comprises my original work. No material in this thesis has been previously published and written by another person, except where due reference is made in the text of the thesis. I further declare that this thesis contains no material which has been submitted for a degree or diploma or other qualifications at any other university.

Signature:

Date: February 5, 2016

A.2 FURTHER STUDIES

Further studies related to this thesis work can be done in the following areas:

(a) Comparison of AoA estimation algorithms.
(b) Design of DF antenna elements.

A.3 PUBLICATIONS FROM THESIS WORK

Academic Journals
- Ozturk, M.E., Korkmaz, E., Kebeli, M., "Rounded-Edge Bow-Tie Antenna for Wideband Mobile Direction Finding System", *IET Microwaves, Antennas & Propagation*, Vol. 2015/9, No. 15, pp. 1751-8733, Dec. 2015.

Conference Proceedings
- Ozturk, M.E., Kebeli, M., "Comparison of Directed Bow-Tie Antenna Types for Direction Finding at UHF", *Proceedings of the 2013 IEEE AP-S International Symposium on Antennas and Propagation & USNC/URSI National Radio Science Meeting*, Orlando (FL) / USA, Jul. 2013.
- Ozturk, M.E., Kebeli, M., "Directed Rounded-Edge Bow-Tie Antenna for Direction Finding at Ultra High Frequencies", *Proceedings of the 2013 IEEE AP-S International Symposium on Antennas and Propagation & USNC/URSI National Radio Science Meeting*, Orlando (FL) / USA, Jul. 2013.

CURRICULUM VITAE

CONTACT INFORMATION
Mehmet Emin ÖZTÜRK
Mimar Sinan Mahallesi, Himmet Baba Sokak, No:31/10 Üsküdar, Istanbul, Turkey
Phone: (0536) 718 33 69
Email: meozturk@gmail.com

EDUCATION
Ph.D., Electrical and Electronics Engineering, Fatih University, Istanbul, Turkey, February 2016
Dissertation: "Development of A Wideband Direction Finding System"

M.S., Electrical and Electronics Engineering, Fatih University, Istanbul, Turkey, August 2009
Thesis: "Effectiveness of Boundary Integral Equations Solution Techniques"

B.S., Electronics Engineering, Fatih University, Istanbul, Turkey, June 2007

PROFESSIONAL EXPERIENCE
- R&D Manager, BCS Tech. & Hitachi Kokusai, Istanbul, Turkey, (2015- Present)
- Researcher, TUBITAK-BILGEM, Kocaeli, Turkey, (2012-2015)
- Research Assistant, Electrical and Electronics Engineering Department, Fatih University, Istanbul, Turkey, (2009 - 2012)

AWARDS AND HONORS
- Received TUBITAK scholarship for PhD. studies in Electrical and Electronics Engineering at Fatih University, (2009 - 2015)
- Received full university scholarship for graduate studies in Electrical and Electronics Engineering at Fatih University, (2007 - 2015)
- Received TUBITAK scholarship for M.S studies in Electrical and Electronics Engineering at Fatih University, (2007 - 2009)
- Received full university scholarship for undergraduate studies in Electronics Engineering at Fatih University, (2002 - 2007)
- Ranked 158th among 1,500,000 students in the National University Admissions Exam (OSS), (2002)

PUBLICATIONS

Books/Book Chapters

- Ozturk, M.E., *Effectiveness of Boundary Integral Equations Solution Techniques with Application*, LAMBERT 12/2011.

Academic Journals

- Ozturk, M.E., Korkmaz, E., Kebeli, M., "Rounded-Edge Bow-Tie Antenna for Wideband Mobile Direction Finding System", *IET Microwaves, Antennas & Propagation*, Vol. 2015/9, No. 15, pp. 1751-8733, Dec. 2015.

Conference Proceedings

- Ozturk, M.E., Kebeli, M., "Comparison of Directed Bow-Tie Antenna Types for Direction Finding at UHF", *Proceedings of the 2013 IEEE AP-S International Symposium on Antennas and Propagation & USNC/URSI National Radio Science Meeting*, Orlando (FL) / USA, Jul. 2013.
- Ozturk, M.E., Kebeli, M., "Directed Rounded-Edge Bow-Tie Antenna for Direction Finding at Ultra High Frequencies", *Proceedings of the 2013 IEEE AP-S International Symposium on Antennas and Propagation & USNC/URSI National Radio Science Meeting*, Orlando (FL) / USA, Jul. 2013.
- Korkmaz, E., Ozturk, M.E., "Comparison of Combined-Field Integral Equation and Constrained Conjugate Gradient Method for Internal Resonance Problem", *Proceedings of the 2010 IEEE AP-S International Symposium on Antennas and Propagation & USNC/URSI National Radio Science Meeting*, Toronto / Canada, Jul. 2010.
- Ozturk, M.E., Korkmaz, E., "Efficiency of Boundary Integral Equation Techniques for Internal Resonans Problem", *Proceedings of the 14th International Symposium on Antenna Technology and Applied Electromagnetics [ANTEM] and the American Electromagnetics Conference [AMEREM]*, Ottowa / Canada, Jul. 2010.

AFFILIATIONS

- IEEE, student member

TECHNICAL SKILLS

- Programming languages: C, CVI, Fortran
- Analytical and statistics programs: Mathematica, MatLab
- Simulation programs: CST MWS, Ansoft HFSS